Chickens Selected for High Body Weight Show Relative Impairment in Fatty Acid Oxidation Efficiency and Metabolic Flexibility in Skeletal Muscle and White Adipose Tissue

by

Shuai Zhang

Thesis submitted to the Faculty of the Virginia Polytechnic Institute and State University in partial fulfillment of the requirements for the degree of

MASTER OF SCIENCE

in

Animal and Poultry Sciences

Elizabeth R. Gilbert, Chair
Mark A. Cline
Matthew W. Hulver
Paul B. Siegel

December 5, 2013
Blacksburg, VA

Key Words: fatty acid oxidation, metabolic flexibility, PDH, *PDK4*, *FoxO1*, *PPARγ*

Chickens Selected for High Body Weight Show Relative Impairment in Fatty Acid Oxidation Efficiency and Metabolic Flexibility in Skeletal Muscle and White Adipose Tissue

Shuai Zhang

ABSTRACT

The ability to adapt fuel usage to nutrient availability is termed metabolic flexibility, and is influenced by activity of the pyruvate dehydrogenase complex (PDC). The Virginia lines of chickens are a unique model of anorexia and obesity that have resulted from 56 generations of artificial selection for high (HWS) or low (LWS) juvenile body weight. We hypothesized that hyperphagia and obesity in juvenile HWS chickens are associated with altered fatty acid oxidation efficiency and metabolic flexibility in tissues associated with energy sensing and storage, and relative cellular hypertrophy in white adipose tissue. Hypothalamus, liver, *Pectoralis major*, gastrocnemius, abdominal fat, clavicular fat and subcutaneous fat were collected from juvenile (56-65 day-old) HWS and LWS chickens for metabolic, gene expression and histological assays. The HWS chickens had reduced fatty acid oxidation efficiency in abdominal fat ($P < 0.0001$) and reduced rates of oxidation in abdominal fat and gastrocnemius ($P < 0.0001$) as compared to LWS. There was reduced citrate synthase activity in white adipose tissue ($P < 0.0001$) and greater metabolic inflexibility in skeletal muscle ($P = 0.006$) of HWS compared to LWS. Greater pyruvate dehydrogenase kinase 4 (*PDK4*) and forkhead box O1 (*FoxO1*) mRNA were found in skeletal muscle and white adipose tissue of 56-day-old HWS than LWS.

Expression of peroxisome proliferator-activated receptor γ (*PPARγ*) in all adipose tissue depots was greater ($P < 0.05$) in LWS than in HWS chickens. The HWS chickens had larger ($P < 0.0001$) and fewer ($P < 0.0001$) adipocytes per unit area than LWS. These results suggest that the HWS chickens have impaired metabolic flexibility and fatty acid oxidation efficiency due to an up-regulation of pyruvate dehydrogenase activity to accommodate the influx of acetyl CoA from fatty acid oxidation in skeletal muscle and white adipose tissue. These metabolic adaptations can be linked to differences in gene expression regulation and body composition between the lines. Adipocyte cellularity data are consistent with greater oxidative efficiency in the adipose tissue of LWS, because of the greater number of unfilled cells in all depots that were sampled. Results can be extrapolated to agricultural production in the understanding of factors regulating the amount of lipid deposition in chicken carcass fat. Results may also provide insight into eating disorders and the development of obesity.

ACKNOWLEDGEMENTS

I would like to take this opportunity to express my gratitude to everyone who helped me during the one and a half years of my graduate study at Virginia Tech. First and foremost, I would like to thank my major advisor, Dr. E. R. Gilbert. I am very grateful for the opportunity provided by Dr. Gilbert for me to pursue a Master's degree in the United States. I'm also very grateful for all of the guidance that she has given me on research, courses and life abroad during the past three semesters. Thank you Dr. Gilbert, for your kindness, encouragement and support! I'm proud to be your graduate student and I'm very eager to start my new PhD life under your guidance!

I also wish to express my sincere gratitude to Dr. P. B. Siegel, Dr. M. A. Cline and Dr. M. W. Hulver for serving on my committee and for their comments and suggestions during my Master's project. I'm deeply impressed by Dr. Siegel's logical thinking and dedication to academia. I'm also inspired by Dr. Cline's enthusiasm as well as his rigorous attitude towards scientific research. All of the knowledge that I gained from Dr. Hulver during the wonderful graduate nutrition course was also a treasure to me. I learned so much from you all!

I would like to also extend my thanks to Dr. R. P. McMillan for his technical experience during this project and intellectual contributions to my manuscripts. I especially thank the Paul B. Siegel Poultry Center Farm Manager, Mike Graham, for his outstanding support of the chicken trials.

Special acknowledgement is extended to my lab colleagues, Lacee Zhang, Lindsay Sumners, Laura Nelson, Dr. Yunjie Tu, Dr. Shiping Bai, Brittany Rice, Doug Gantt,

Guoqing Wang, Jiaqing Yi and undergraduates for helping me with the chicken trials, as well as for their patient discussion, suggestions and encouragement. I'm also indebted to Dr. E. A. Wong, and his lab members, Huadong Yin and Shengchen Su, for generously helping me with my Master's project. Thank you, Dr. Wong for serving as my co-advisor with Dr. Gilbert during my PhD program!

I'm also indebted to the entire faculty and staff in the Animal and Poultry Sciences Department for their help with my study. I would also like to thank my friends in Blacksburg: Fan He, Yu Zhou, Ming Xie, Qian Cao, Qinghui Mu, Lei Deng, Xin Feng and so on.

I most appreciate my parents, for giving me the gift of life. Thanks for your understanding and support for me to study abroad, and all of the encouragement throughout my academic endeavors. I would not be able to complete my graduate studies without your help!

TABLE OF CONTENTS

LIST OF TABLES

LIST OF FIGURES

ABBREVIATIONS

AMPK	**5’-AMP-activated protein kinase**
Ang II	**Angiotensin II**
ASM	**Acid soluble metabolites**
CD36	**Cluster of differentiation 36**
CPT1	**Carnitine palmitoyl-coenzyme A transferase 1**
CS	**Citrate synthase**
DCA	**Dichloroacetate**
DHAP	**Dihydroxyacetone phosphate**
DTNB	**5,5'-Dithiobis-2-Nitrobenzoic Acid**
eIF4E	**Eukaryotic initiation factor 4E**
ERRα	**Estrogen related receptor α**
FAT	**Fatty acid transporter**
FFA	**Free fatty acid**
FoxO	**Forkhead box protein O**
G3P	**Glycerol 3-phosphate**
GH	**Growth hormone**
GSIS	**Glucose simulated insulin secretion**
HWS	**Chickens from lines selected for high body weight**
IRS 1/2	**Insulin receptor substrates 1 and 2**
INS-1E	**Insulinoma E**
LCFA	**Long-chain fatty acids**
LXR	**Liver X receptor**

LWS	**Chickens from lines selected for low body weight**
MAPK	**p38 mitogen-activated protein kinase**
PDC	**Pyruvate dehydrogenase complex**
PDH	**Pyruvate dehydrogenase**
PDK	**Pyruvate dehydrogenase kinase**
PEPCK	**Phosphoenolpyruvate carboxykinase**
PGC1α	**PPARγ co-activator 1α**
PI3K	**Phosphoinositide 3-kinase**
PPAR	**Peroxisome proliferator-activated receptor**
ROS	**Reactive oxygen species**
SHP	**Small heterodimer partner**
STAT5	**Signal transducer and activator of transcription 5**
T2DM	**Type 2 diabetes mellitus**
TAG	**Triacylglycerol**
TCA	**Tricarboxylic acid**
TR	**Thyroid hormone receptor**
TZD	**Thiazolidinediones**
WAT	**White adipose tissue**

CHAPTER 1 Introduction

The prevalence of obesity has reached epidemic proportions with at least one third of all US adults considered to be overweight or obese (CDC, 2012). This trend is expected to continue, with rising health costs associated with the treatment of obesity and its comorbidities such as heart disease, stroke, type 2 diabetes and certain types of cancer (Poirier et al., 2006). Obesity involves a combination of chronic elevations in caloric intake and enhanced storage of energy in the form of triglycerides in white adipose tissue. The hypothalamus-adipose tissue axis has been well described in mammals, in which factors released by both the white adipose tissue and hypothalamus can affect energy sensing status and expenditure of both tissues, and thereby modulate whole body energy balance (Schaffler et al., 2005; Shimizu and Mori, 2005; Morton et al., 2006; Breton, 2013). Thus, research on the molecular regulation of appetite, feeding behavior and energy expenditure and storage in hypothalamus and insulin-dependent tissues such as skeletal muscle and white adipose tissue may provide valuable insights on the mechanisms underlying appetite and body composition.

The chicken is a versatile model organism that bridges the evolutionary gap between mammals and other vertebrates. The Virginia lines of chickens are a unique model of anorexia and obesity that have resulted from long-term divergent selection for high (HWS) or low (LWS) body weight. These chickens have been selected for 56 generations with complete pedigrees that go back to the original founder population of White Plymouth Rocks. Selection for body weight has been associated with correlated responses in feeding behavior and body composition, whereby the LWS are lean and

some anorexic, while the HWS are over-eaters and become obese as juveniles (Dunnington and Siegel, 1996; Dunnington et al., 2013). Calabotta et al. (1984) examined lipogenic and lipolytic capacities in fasted and non-fasted 28-day-old HWS and LWS chickens (Calabotta et al., 1985). Regardless of the feeding state, LWS chickens exhibited greater lipogenic capacities in liver and bone tissues and higher lipolytic capacities in abdominal adipose tissue as compared to their HWS counterparts (Calabotta et al., 1985). The rate of lipolysis exceeded the rate of lipogenesis, explaining, in part, why the LWS had little fat accumulation. Administration of nutrients by oral gavage was associated with minimal fat deposition in the LWS, which occurred primarily through hypertrophy, whereas adipose tissue expansion in the HWS was through a combination of hyperplasia and hypertrophy (Robey et al., 1988; Robey et al., 1992). Collectively, these studies suggest that there is a greater capacity to efficiently and rapidly oxidize lipids in the LWS as compared to HWS and that fat deposition in anorexic and obese animals occurs through different cellular mechanisms.

The underlying mechanisms in the complex network that regulates energy homeostasis are critical to understand in the research of obesity and metabolic syndrome. Large numbers of pathways and chemicals are involved in this network and interact with each other intricately. Because of differences in feeding behavior and body composition between the lines, fatty acid oxidation and metabolic flexibility might provide a link between energy intake and expenditure. In the present study, body weights differed by more than tenfold between the lines, with extensive fat deposition in HWS and almost no visible fat accumulation in LWS at any age studied. Differences in metabolism were

observed as were expression levels of several metabolism-associated factors in hypothalamus, adipose tissue and skeletal muscle.

We hypothesized that hyperphagia and obesity in juvenile HWS chickens are associated with reduced fat oxidation efficiency and metabolic inflexibility in adipose tissue and skeletal muscle, and relative cellular hypertrophy in white adipose tissue. The objective of this study was to evaluate fatty acid oxidation and metabolic flexibility in different tissues of juvenile LWS and HWS chickens. We evaluated abundance of *PDK4*, *FoxO1*, *PPARγ* and *PGC1α* mRNA as markers related to metabolic flexibility in different tissues of 28- and 56-day old LWS and HWS chickens. Because obesity is also associated with cellular changes in adipose tissue, we measured adipocyte cellularity in different fat depots of LWS and HWS individuals.

Information from this study may be useful in elucidating the factors regulating lipid deposition in chicken carcass fat in agricultural production. The understanding of adipose development and appetite regulation have the potential to benefit human beings by providing information that can be used to improve body composition and reduce the occurrence of obesity and metabolic disorders.

CHAPTER 2 Literature Review

2.1 Introduction

This review summarizes the recent studies on PDKs pivotal role in controlling metabolic flexibility, a recent concept in cellular energy metabolism, in various nutritional conditions (such as energy deprivation, high fat diet, exercise and diseases) in diverse tissues (such as skeletal muscle, liver, adipose tissue, heart, pancreatic islets and nervous system), with emphasis on the best characterized PDK4. Understanding the regulation of PDKs in different tissues and their role in energy homeostasis will be beneficial for treatment of different kinds of metabolic diseases.

2.2 Metabolic flexibility

Maintaining a balance between energy demand and supply is critical for health. Glucose and lipids (fatty acids and ketone bodies), as sources of cellular energy, can compete and interact with each other (Randle, 1998). The capacity for an organism to adapt fuel oxidation to fuel availability, that is, to preferentially utilize carbohydrate and lipid fuels and to be able to rapidly switch between them is termed metabolic flexibility (Storlien et al., 2004; Galgani et al., 2008). The failure to match fuel oxidation to changes in nutrient availability is often accompanied by symptoms such as insulin resistance, ectopic lipid accumulation and mitochondrial dysfunction (Galgani et al., 2008; Sugden et al., 2009). Thus, metabolic inflexibility is tightly related to a series of syndromes such as type 2 diabetes mellitus, obesity, cardiovascular disease and metabolic syndrome.

2.3 PDC and PDKs

One of the major enzymes responsible for linking glucose and fatty acid metabolism in mammals is the pyruvate dehydrogenase complex (PDC), a mitochondrial multi-enzyme complex that catalyzes the oxidative decarboxylation of pyruvate (Gudi et al., 1995). PDC controls the conversion of pyruvate, Coenzyme A (CoA) and NAD^+ into acetyl-CoA, NADH and CO_2, thus links fatty acid oxidation, glycolysis, gluconeogenesis and the tricarboxylic acid (TCA) cycle (Sugden and Holness, 2006). The CoA-activated two-carbon unit produced by the catabolism of pyruvate can be condensed with oxaloacetate in the first reaction of the TCA cycle, or used for fatty acid and cholesterol synthesis (Strumilo, 2005). The three-carbon compounds may also be conserved for gluconeogenesis in liver and kidney (Huang et al., 2003). Thus, the PDC occupies a central position in cellular metabolism (Figure 2.1).

PDC is normally active in the healthy and well-fed state. However, suppression of PDC is crucial for glucose synthesis when glucose is scare (Sugden, 2003). The inactivation of PDC activity is catalyzed by four highly specific pyruvate dehydrogenase kinase (PDK) isozymes that can phosphorylate specific serine residues within the α subunit of the E1 enzyme in the PDC (Sugden and Holness, 1994; Gudi et al., 1995). Of all the known isozymes, *PDK2* and *PDK4* are the most widely distributed and are highly expressed in heart, liver and kidney in humans and rodents. *PDK4* is also abundant in pancreatic islets and in skeletal muscles that have high fatty acid oxidation rates. *PDK1* and *PDK3* have rather limited tissue distribution (Holness and Sugden, 2003). The PDKs activities can be regulated by different levels of metabolites as well as transcription factors under various conditions and in different tissues (Figure 2.2). Thus the PDC can

manage the use and storage of fuels to fulfill metabolic flexibility in response to the environment.

2.4 The pivotal role of PDKs in metabolic flexibility

2.4.1 Skeletal muscle

As quantitatively the largest organ in the body, skeletal muscle accounts for 30% to 40% of the metabolic rate in adults in the resting state. Contributing to 80% of insulin-stimulated glucose uptake, it is a major site for fatty acid and glucose oxidation (de Lange et al., 2007). The skeletal muscle exhibits remarkable metabolic flexibility in fuel usage in response to various metabolic challenges such as energy deprivation and changes in diet composition. In lean healthy individuals, skeletal muscle is able to switch from predominantly lipid oxidation and high rates of fatty acid uptake to the suppression of lipid catabolism and elevated glucose uptake, oxidation and storage under insulin stimulation (Kelley and Mandarino, 2000). However, obese and T2DM patients manifest greater rates of lipid oxidation in skeletal muscle and relatively insulin resistant, resulting in metabolic inflexibility (Kelley and Mandarino, 2000).

2.4.1.1 Energy deprivation

In times of energy deprivation, glucose is scarce and long-chain fatty acid (LCFA) oxidation is used to meet cellular energy requirements. Reduced food intake and lowered insulin concentrations decrease glucose utilization to conserve glucose (Sugden and Holness, 2006). Mammalian PDC activity is suppressed by PDK's hyper-phosphorylation, limiting the conversion of pyruvate to acetyl-CoA in skeletal muscle (Holness and Sugden, 2003). Fatty acid oxidation is both forced and facilitated by up-regulation of

PDK4 (Sugden et al., 2000). Short-term fasting (complete food withdrawal) (48h) was associated with a 3-4 fold increase in PDK4 protein and mRNA in gastrocnemius muscle in rats, with no effects on *PDK2* expression (Wu et al., 1999). However, energy deprivation led to a decrease rather than increase in PDK2 activity in gastrocnemius muscle in *PDK4* knock-out mice. This suggested PDK2 cannot compensate the function of PDK4 in the absence of PDK4 in response to fasting (Jeoung et al., 2006). The fasted *PDK4* knock-out mice exhibited lowered blood glucose, elevated serum non-esterified fatty acids and greater PDC activity in gastrocnemius muscle (Jeoung et al., 2006), consistent with the lower rates of fatty acid oxidation and increased rates of glucose and pyruvate oxidation. Refeeding the fasted rats for 48h reduced *PDK4* mRNA to a level comparable to the control group (Wu et al., 1999).

The acetyl-CoA and NADH produced by fatty acid oxidation stimulated PDK activity in skeletal muscle (Holness and Sugden, 2003). There was also a selective induction of *FoxO1* (forkhead box O1) and *FoxO3* (forkhead box O3) transcripts in gastrocnemius muscle in mice after 48h of food withdrawal (Furuyama et al., 2003), indicating the involvement of the *FoxO* in up-regulation of *PDK4* in response to short-term changes in nutritional state. *PDK4*, interacting with fatty acid transporter/cluster of differentiation 36 (FAT/CD36, major fatty acid uptake proteins in muscle), peroxisome-proliferator activated δ/β (*PPARδ/β*, fatty acid activated nuclear receptor) and *FoxO1*, provides a framework for regulating muscle fuel preference in response to fasting (Nahle et al., 2008). During energy deprivation, CD36-facilitated fatty acid flux activates *PPARδ/β*, which coordinately produces increases in *FoxO1* and *PDK4* expression to inhibit glucose oxidation. Since *FoxO1* also recruits CD36 to the plasma membrane and

induces lipoprotein lipase, all of these enhanced fatty acid utilization in skeletal muscle (Nahle et al., 2008). The novel liver X receptor (*LXR*)-*PPARα* metabolostatic signaling axis was also reported to be involved in the muscle energy deprivation response (Kase et al., 2005; Caton et al., 2011). The activation of *LXR* augmented *PPARα* signaling to increase fasting-induced up-regulation of *PDK4* expression, thus enhancing fatty acid oxidation and decreasing glucose catabolism in skeletal muscle (Kase et al., 2005; Caton et al., 2011).

2.4.1.2 Long-term high fat diet consumption

Long-term consumption of a high-saturated fat diet may cause hyperglycemia, hyperinsulinaemia, glucose intolerance and obesity. The administration of a diet high in saturated fats for 4 weeks to rats significantly increased PDK2 and PDK4 protein expression in both fast-twitch (anterior tibialis) and slow-twitch (soleus) muscles in rats (Holness et al., 2000). In soleus, the relative increase in *PDK4* expression was also linked to a more than 7 fold increase in pyruvate concentration and a 50% reduction in PDC activity compared to that in anterior tibialis (Holness et al., 2000), indicating greater insulin sensitivity in slow-twitch muscle compared to fast-twitch muscle. Consumption of a high fat diet leads to the use of lipid-derived fuels as respiratory substrates in muscle, in part modulated by the up-regulation in PDK activity. The enhanced fatty acid oxidation after feeding high fat diets in slow-twitch muscle is mainly attributed to the up-regulation of *PDK4*. However, in fast-twitch muscle, increased *PDK2* mRNA expression was also observed (Holness et al., 2000), suggestive a possible coordinate regulation between *PDK2* and *PDK4* in white muscle fiber sub-types.

PDK4 deficiency leads to decreased fatty acid oxidation and increased glucose oxidation due to less inhabitation of PDC activity. However, feeding high-fat diets in the long term didn't further promote ectopic fat accumulation and worsen insulin resistance (Jeoung and Harris, 2008; Hwang et al., 2009). After feeding a high-saturated fat diet for 32 weeks, the *PDK4* deficient mice also developed hyperinsulinaemia, but less fat accumulation in skeletal muscle and better glucose tolerance as compared to the wild-type mice (Hwang et al., 2009). The fatty acid synthase activity was also lower, suggesting the absence of *PDK4* may alter signaling components involved in regulation of lipid metabolism (Hwang et al., 2009).

Up-regulation of the orphan nuclear receptor ERRα (estrogen related receptor α) mRNA and protein was found in mice after chronic consumption of a high-fat diet (Rinnankoski-Tuikka et al., 2012). It has been suggested that peroxisome proliferator-activated receptor γ coactivator 1α (*PGC-1α*) can regulate glucose catabolism and mitochondrial oxidative pathways by increasing PDK4 activity via a *PGC1α/ERRα* dependent pathway in skeletal muscle (Wende et al., 2005; Connaughton et al., 2010). *ERRα* can recruit *PGC1α* to the *PDK4* promoter, which is independent of *FoxO1* and *PPAR*s (Araki and Motojima, 2006). The negatively regulation of PDC activity by PDK4 inhibits the entry of pyruvate into the TCA cycle and subsequently blunts cellular glucose oxidation in response to high-fat feeding (Rinnankoski-Tuikka et al., 2012). Thus *PGC1α/ERRα* has a key role in high fat diet induced *PDK4* up-regulation and metabolic flexibility in skeletal muscle.

2.4.1.3 Exercise

It was found that PDC activation during low to moderate-intensity muscle contraction was ~2 fold higher in *PDK4* knockout mice than in wild-type mice during exercise, regardless of the intensity (Herbst et al., 2012). *PDK4* mRNA was markedly increased during prolonged exercise and after both short-term high-intensity and prolonged low-intensity exercise in skeletal muscle in mice (Pilegaard and Neufer, 2004). The inactivation of PDC in response to both slow-twitch and fast-twitch muscle contraction through up-regulated *PDK4* can limit the entry of glycolytic products into the mitochondria for oxidation. The recovery period after exercise also highlights the high metabolic priority of glycogen replenishing to re-establishing the energy homeostasis in skeletal muscle (Pilegaard and Neufer, 2004). High fat diet consumption followed by exercise also elevated *PDK4* expression in human skeletal muscle (Constantin-Teodosiu et al., 2012), leading to reduced PDC activity and less carbohydrate oxidation. *FoxO1* was suggested to be a possible factor related to this change. *FoxO1* can sense changes in availability of free fatty acids, and relay this message downstream by modulating transcription of *PDK4* (Constantin-Teodosiu et al., 2012). *PGC-1α* also played significant roles in skeletal muscle in response to exercise according to research on horses (Eivers et al., 2012). PGC1α regulated glucose oxidation while increasing mitochondrial respiration and fatty acid oxidation during post-exercise recovery in Thoroughbred horses (Eivers et al., 2012).

In addition to exercising muscle, during acute endurance exercise in the one-leg cycling model, the resting muscle also showed increased *PDK4* expression, likely mediated by elevation in circulating free fatty acids, ligands of *PDK4*, and up-regulation of *PPAR*s pathways (Catoire et al., 2012).

2.4.1.4 Insulin resistance and diabetes

Insulin resistance is most characterized as a limited response of skeletal muscle to stimulated glucose metabolism. Also the resistance to suppression of lipid utilization under insulin resistance impaired the capacity to switch between fuels, leading to metabolic inflexibility (Kelley and Mandarino, 2000). This is common for obese and type 2 diabetes patients during insulin stimulated conditions. Kim et. al (2006) induced acute insulin resistance by constant infusion of Intralipid (a fat emulsion) and lactate for 5h in rats, resulting in 2 to 3 fold higher *PDK4* expression in muscle following insulin infusion, indicating the impaired ability of insulin to suppress *PDK4*. The Intralipid and lactate infusion also decreased the phosphorylation of *Akt* and *FoxO1*, illustrating the impaired insulin signaling (Kim et al., 2006). A more recent clinical research study showed that growth hormone (GH) can promote lipolysis and reduce insulin sensitivity in human subjects. This was associated with up-regulation of *PDK4* mRNA and decreased active PDC, similar to what is observed during fasting (Nellemann et al., 2013). The research on type 2 diabetes mellitus (T2DM) patient muscle biopsies showed that both *PDK2* and *PDK4* mRNA were increased in comparison to healthy patients after overnight fasting (Kulkarni et al., 2012), which was consistent with the insulin resistance and metabolic inflexibility of T2DM patients. Furthermore, methylation status of cytosines in the +160 and +446 region of the *PDK4* promoter was reduced in T2DM patients, suggesting that epigenetic modification of mitochondrial genes are involved in regulating substrate switching (Kulkarni et al., 2012). However, as one of the transcriptional factors that regulates expression of *PDK4*, *PGC1α* was reported to be hyper-methylated in skeletal muscle of type 2 diabetic human subjects (Barres et al., 2009) and after fat overfeeding

low birth weight individuals (Brons et al., 2010), indicating that altered methylation patterns associated with metabolic disease may be promoter specific (Kulkarni et al., 2012).

Therapeutic interventions have been used to reduce *PDK4* expression in diabetes. Beyond insulin, several PDK4 inhibitors were utilized to promote glucose disposal in animal models. Initial studies showed encouraging results with oral administration of dichloroacetate (DCA), but this compound is a weak PDK inhibitor and toxic (Stacpoole et al., 1998). More recently, the potent oral administration of drugs such as PDK inhibitors produced by Novartis and AstraZeneca usually include amides of trifluoro-2-hydroxy-2-methylpropionic acid (Roche and Hiromasa, 2007). All of these inhibitors, including the PDK2 inhibitor Nov3r and AZD7545, bind at the lipoyl group binding site of PDK and effectively increase PDC activity (Roche and Hiromasa, 2007). Many drugs target the PDK activity in most peripheral tissues, like DCA (Roche and Hiromasa, 2007), but some drugs have better efficacy in specific tissue. For example, AZD7545 elevated PDC activity more effectively in liver than in skeletal muscle and heart and with the loss of efficacy in skeletal muscle of fasted animals (Morrell et al., 2003).

2.4.2 Liver

One of the primary functions of liver is to regulate the supply of glucose and other metabolic fuels to provide energy to other tissues (Gross et al., 2008). The body can balance the blood glucose levels through balancing glucose production and storage in liver and in kidney, and regulating its utilization in peripheral tissues. Under fasting conditions, the liver initially provides glucose from glycogenolysis, the breakdown of liver glycogen stores. With prolonged energy deprivation, the primary glucose source is

gluconeogenesis, the synthesis of glucose from non-carbohydrate precursors such as glycerol, lactate and the amino acid alanine (Gross et al., 2008). Inactivation of PDC by PDKs can inhibit conversion of pyruvate to acetyl-CoA, resulting in a shift of pyruvate to the TCA cycle or toward gluconeogenesis (Randle, 1986).

Fasting for 48h did not alter PDC activity in the liver of *PDK4* knockout mice, but intermediates of the gluconeogenic pathway (glucose 6-phosphate, fructose 1,6-bisphosphate, pyruvate, lactate and citrate) were lower (Jeoung et al., 2006), indicating a reduced rate of gluconeogenesis and glycolysis. Growth hormone (GH) can increase hepatic *PDK4* expression in liver in wild-type mice during fasting through the activation of Signal transducer and activator of transcription 5 (STAT5), leading to inhibition of PDC activity, conserving substrates for gluconeogenesis (Kim et al., 2012). Metformin, a commonly prescribed drug for T2DM, can inhibit GH-induced *PDK4* expression via a 5'-AMP-activated protein kinase - small heterodimer partner (*AMPK-SHP*) dependent pathway to inhibit the combination of STAT5 to *PDK4* promoter (Kim et al., 2012).

Hepatic expression of the *PDK4* and *PDK2*, and PDC activity were not affected in wild-type mice fed a high-fat diet for 18 weeks. (Jeoung and Harris, 2008). High-fat diet feeding induced hepatic steatosis, a condition that occurs when fat accumulation exceeds the oxidation rate (Jeoung and Harris, 2010). This situation was prevented in *PDK4* knockout mice that consumed a high-saturated fat diet for 32 weeks (Hwang et al., 2009). This can be explained in part by the altered PGC1α activity in the liver. PGC1α controls expression of gluconeogenic enzymes such as phosphoenolpyruvate carboxykinase (PEPCK). Knocking out *PDK4* could lead to higher levels of PGC1α, consistent with greater activity of PEPCK and a lower capacity for *de novo* fatty acid synthesis (Hwang

et al., 2009). *PPARα* also showed coordinated regulation with *PGC1α* in hepatic steatosis, which was demonstrated by the enhanced beneficial effects of clofibric acid, a *PPARα* agonist, on fatty acid accumulation in *PDK4* knockout mice (Hwang et al., 2012). In contrast to skeletal muscle, FAT/CD36, key enzymes for fatty acid transport, were not involved in the reduced fat accumulation in liver (Hwang et al., 2009).

Under diabetic conditions, expression of the *PDK* genes, particularly *PDK4*, are significantly elevated in the liver, which could help explain the increased rates of gluconeogenesis (Tao et al., 2013), and the beneficial effects of metformin. Research on the diabetic mice model that is deficient in hepatic insulin receptor substrates 1 and 2 (*IRS 1/2*) revealed that both knockdown and knockout of the *PDK4* gene led to improvement of glycemic control and glucose tolerance. *PDK4* was more efficient in regulating metabolic flexibility than *PDK2* in liver (Tao et al., 2013). Combined with the results from the other studies, it seems that *PDK2* mainly regulates glucose utilization whereas *PDK4* may be involved in both system glucose metabolism and hepatic gluconeogenesis.

2.4.3 White adipose tissue

Compared to the skeletal muscle and liver, relatively little research is reported on metabolic flexibility in white adipose tissues (WAT). WAT is a crucial organ for fatty acid metabolism, a process referred as adipocyte glyceroneogenesis. This pathway uses pyruvate, alanine, glutamine or any substances from the TCA cycle as precursors to synthesize dihydroxyacetone phosphate (DHAP) and finally to produce glycerol 3-phosphate (G3P) for triacylglycerol (TAG) synthesis (Nye et al., 2008). Thus PDC is

linked to this process and suppression of PDC allows increased use of lactate and pyruvate for glyceroneogenesis (Holness et al., 2012).

As an activator of glyceroneogenesis, thiazolidinediones (TZD) increased *PDK4* mRNA expression in subcutaneous, periepididymal and retroperitoneal WAT depots in genetic obese, insulin resistant rats, while *PDK2* mRNA was not affected, indicating the vital role of *PDK4* in glyceroneogenesis. TZD induction of PDK4 expression was tissue-specific because liver and muscle did not respond to such a treatment (Cadoudal et al., 2008). Similar results were observed for 3T3-F442A adipocytes in vitro, using *PDK4* inhibitors, DCA and leelamine, and *PDK4* siRNA. Both 500 μmol/L DCA and 50 μmol/L leelamine inhibited pyruvate incorporation into triglycerides. Incorporation of [1-^{14}C] pyruvate into lipids was reduced 40% after transfection of adipocytes with *PDK4* siRNA (Cadoudal et al., 2008). Peroxisome proliferator-activated receptor γ (PPARγ) is a nuclear receptor regulated by the insulin-sensitizing TZDs. PDK4 is an indirect target of PPARγ. Thus the regulation of PDK4 by TZD in WAT tightly relates to PPARγ (Sears et al., 2007).

Apart from TZD, acute epinephrine treatment also increased *PDK4* mRNA through p38 mitogen-activated protein kinase (*MAPK*) and *AMPK* pathways in cultured adipose tissue (Wan et al., 2010) and in WAT in obese, insulin resistant rat models that were induced to become obese by high fat diets (Wan et al., 2012). *PDK2* mRNA was still unaffected. Two hours of swimming produced similar results as epinephrine treatment in WAT in both lean and obese rats (Wan et al., 2012). Combined with increased glycerol-3-phosphate (G3P) synthesis via PEPCK, more glyceroneogenesis allows increased re-esterification of non-esterified fatty acids into TAG from lipolysis,

while glucose oxidation is reduced in these adipocytes (Wan et al., 2010). With a major role in glucose clearance and fat synthesis/storage, up-regulation of *PDK4* during exercise, epinephrine and TZD treatment leading to PDC inhibition, promotes energy storage in WAT. More work is needed for the transcriptional pathways involved in PDK4 up-regulation in WAT (Jeong et al., 2012).

2.4.4 Heart

Metabolic inflexibility always accompanies cardiomyopathy, particularly during ischemia, and may even cause heart failure (Roche and Hiromasa, 2007). Failure to oxidize enough carbohydrate to meet energy demands is an important reason for cardiac inefficiency. This can be demonstrated by cardiac-specific overexpression of *PDK4*, which is sufficient to cause a loss of metabolic flexibility and exacerbate cardiomyopathy (Zhao et al., 2008). Overexpression of *PDK4* in heart with a transgenic mouse model was associated with a decrease in glucose catabolism and a corresponding increase in fatty acid oxidation. This transgenic model also expressed a constitutively active form of the phosphatase calcineurin, and thus caused hypertrophy in cardiomyocyte fibrosis and a striking increase in mortality (Zhao et al., 2008).

In mice that were fed a high fat diet for 10 days, the cardiac carbohydrate oxidation markedly decreased, with up-regulation of PDK4 activity. The high fat diet induced cardiac metabolic alterations through the eukaryotic initiation factor 4E (*eIF4E*)/*cyclin D1*/*E2F1/PDK4* pathway (Zhang et al., 2012).

During moderately severe ischemia, free fatty acids are the primary fuel in mitochondrial oxidation (Randle, 1986). While glycolysis is still active, the inactivation

of PDC facilitates fatty acid use. Ischemia causes pyruvate to be converted to lactate, thereby increasing the acidification within the myocardium (Roche and Hiromasa, 2007). Thus inhibition of PDK activity by DCA is vital to increase the ATP production as well as the Ca^{2+} uptake, and use of the combination of glucose-insulin-K^{+} or fatty acid oxidation inhibitors are also beneficial (Roche and Hiromasa, 2007).

Angiotensin II (Ang II), the main effector in the renin angiotensin system (RAS) in heart failure, can induce marked cardiac insulin resistance, leading to the cardiac metabolic switch from glucose to fatty acid oxidation, producing metabolic inflexibility and cardiac inefficiency (Mori et al., 2013). *PDK4* is highly expressed in this Ang II induced hypertrophy model and deletion of *PDK4* prevents the Ang II induced reduction in glucose oxidation and prevents diastolic dysfunction (Mori et al., 2013). Inhibition of PDK4 activity has become a new therapeutic strategy against heart disease (Roche and Hiromasa, 2007).

2.4.5 Central nervous system

The brain also takes advantage of glucose oxidation as the primary energy source. Cultured astrocytes expressed more *PDK2* and *PDK4* compared to neurons, consistent with the lower PDH activity and higher lactate production displayed by cultured astrocytes (Jha et al., 2012). There is accumulating evidence that alterations in PDKs activity are linked to the development of several neurological disorders. For instance, Alzheimer's disease was associated with dysfunction in PDH activity and glucose metabolism (Yao et al., 2009). Brain aging is associated with reduced *PDK1* and *PDK2* mRNA in the cerebellum and elevated *PDK2* mRNA in the hippocampus and cerebral

cortex (Nakai et al., 2000), and *PDK2* mRNA up-regulation was involved in glioblastoma (Michelakis et al., 2010).

Hypothalamic neurons are sensitive to nutritional signals and can regulate energy balance and glucose homeostasis. However, the underlining complex mechanisms are still not completely understood. Recent studies on mice fasted for 48h revealed a gene expression profile in hypothalamus consistent with reduced glucose utilization and increased lipid oxidation, including elevated *PDK4* mRNA, consistent with the results in skeletal muscle, liver, heart and kidney (Poplawski et al., 2010). The up-regulation of *PDK4* was also observed in hypothalamus during neonatal rat fasting for 6h, reflecting an attempt to conserve energy during neonatal food deprivation. This also indicates that the neonatal brain is not spared from glucose restriction during energy crisis, but instead the neonatal brain can use ketones derived from fatty acid metabolism as the major source of energy (Ding et al., 2010). However, only limited studies are reported for PDK's effect on hypothalamic energy balance, so more researches are expected.

2.4.6 Pancreatic islets

In murine pancreatic β cells, both high fatty acid and high glucose treatment increased PDK activity and decreased PDH activity. Palmitate up-regulated mRNA expression of *PDK1*, *PDK2* and *PDK4*, while high glucose increased *PDK1*, *PDK2* mRNA but reduced *PDK4* mRNA (Xu et al., 2006), suggestive of different transcriptional regulation. Thus the induction of PDK expression by both glucose and fat contributes to the decline in β cell metabolism flexibility during the progression from obesity to T2DM (Xu et al., 2006).

Chronic exposure to hyperglycemic conditions results in glucotoxicity in β cells. Glucotoxicity impairs glucose simulated insulin secretion (GSIS), contributing to the development of T2DM. Metabolomic analysis of β cells after exposure to high glucose (25mM for 20h) revealed an increase in glucose and decrease in fatty acid during GSIS, but no significant changes in PDK2 protein (Wallace et al., 2013). Similar research on insulinoma E (INS-1E) β cell lines showed an increase in PDC E1α subunit phosphorylation during high glucose treatment (50mM for 48h). Knockdown of PDK1 and PDK3 led to a marked reduction in PDC inactivation. However, the PDC inactivation was not associated with altered GSIS (Akhmedov et al., 2012). It is possible that PDC activity in INS-1E β cells is in excess and therefore lowering its activity is of little consequence. Prolactin can also induce GSIS in INS-1 cell lines by suppression of PDKs and increased PDC activity, suggestive a novel role for lactogens in diabetes treatment (Arumugam et al., 2010). As the most important organ involved in the pathogenesis of T2DM, more research on metabolic flexibility in pancreatic β cells is needed.

2.4.7 Cancer cells

Cancer cells have a unique way to acquire energy, termed the Warburg effect. They utilize increased glycolysis and suppress mitochondrial glucose oxidation to provide energy with a proliferative advantage, conducive to apoptosis resistance and even increased angiogenesis (Hsu and Sabatini, 2008). In low nutrient conditions, the Warburg effect was enhanced through a mechanism involving reactive oxygen species (*ROS*)/*AMPK*- dependent activation of *PDK* (Wu et al., 2013). PDK1 and PDK3 are the main isoforms related to the Warburg effect (Roche and Hiromasa, 2007). Thus inhibition of *PDK* with either small interfering RNAs or orphan drugs, such as DCA, can shift the

metabolism of cancer cells from glycolysis to glucose oxidation, and may provide a powerful approach to treat cancer (Sutendra and Michelakis, 2013).

2.5 Summary

As the major fuels for substrate oxidation to provide energy in birds and mammals, glucose and fatty acids can compete with each other at the level of PDC. PDC is normally active in most tissues in the well-fed state. However, suppression of PDC activity by PDKs is crucial to provide pyruvate and other three-carbon compounds for glucose synthesis when glucose is in demand. PDKs play a pivotal role in stable substrate switching and energy homeostasis, which is known as metabolic flexibility, especially under some extreme nutrient conditions.

The alteration of PDKs expression, particularly *PDK4*, has a tremendous influence on the health status of the organism. Inhibition of PDK4 can benefit specific tissues, such as skeletal muscle, liver and heart, but up-regulation of PDK4 is beneficial in white adipose tissue in obesity and insulin resistance in mice. This can be due to tissue-specific physiology. Glucose is the major fuel source for most tissues, inhibition of PDK4 thereby leading to PDC activation and more glucose oxidation. As the major lipid storage organ, white adipose tissue can take advantage of fatty acids as an energy source, thus increased glyceroneogenesis caused by up-regulated *PDK4* is beneficial. The tissue-specific physiology also involves diverse transcriptional regulation pathways, involving factors such as *FoxO* and *PPARs* (Figure 2.2).

Metabolic inflexibility, combined with abnormal PDKs activity, is directly associated with many diseases, such as type 2 diabetes mellitus, obesity, metabolic

disorders, cardiomyopathy, neurological disorders and several cancers. Future research on PDC and PDKs regulation in various conditions and different tissues will be beneficial to alleviate metabolic inflexibility and to provide possible therapies for numerous diseases.

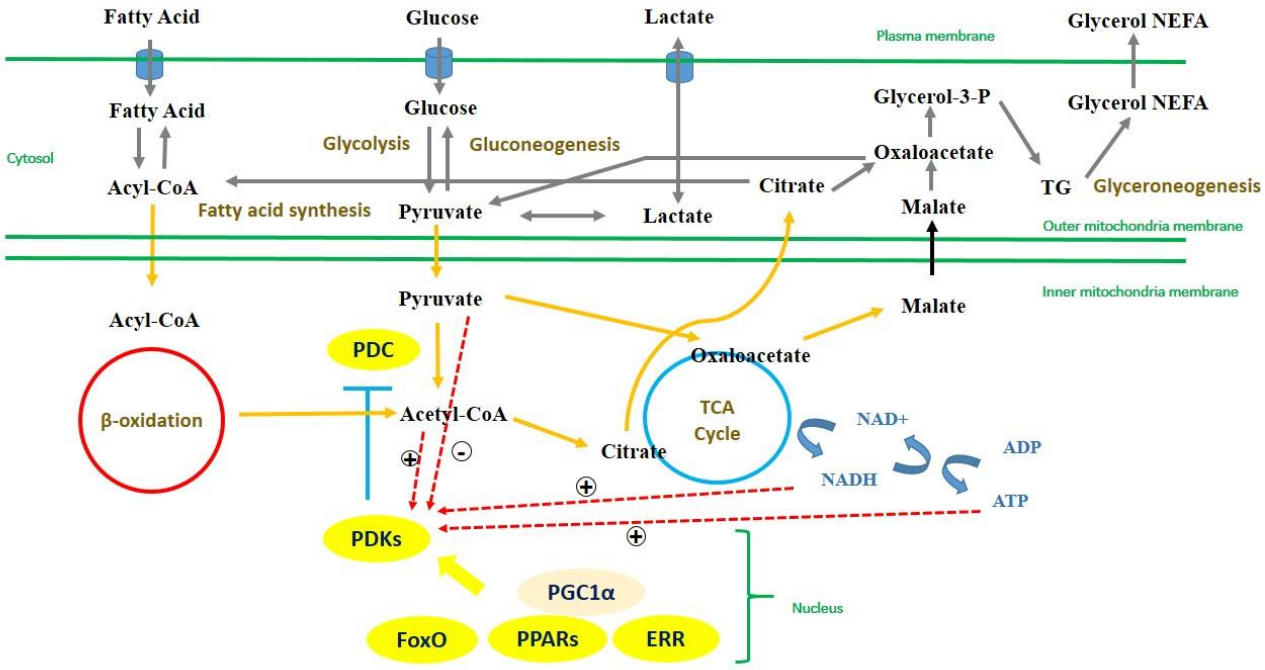

Figure 2.1 Schematic representation of fatty acid and glucose competition for oxidation at the level of the PDC and factors that regulate PDKs. PDC can catalyze the oxidative decarboxylation of pyruvate to form acetyl-CoA and thus links glucose metabolism and fatty acid metabolism. PDC can be phosphorylated by PDK, which can be regulated by mitochondrial acetyl-CoA, NADH, pyruvate, ATP and nuclear transcription factors. PDC: pyruvate dehydrogenase complex. PDKs: pyruvate dehydrogenase kinases. FoxO: Forkhead box protein O. PPAR: peroxisome proliferator-activated receptor. ERR: estrogen related receptor. PGC1α: PPARγ co-activator 1α.

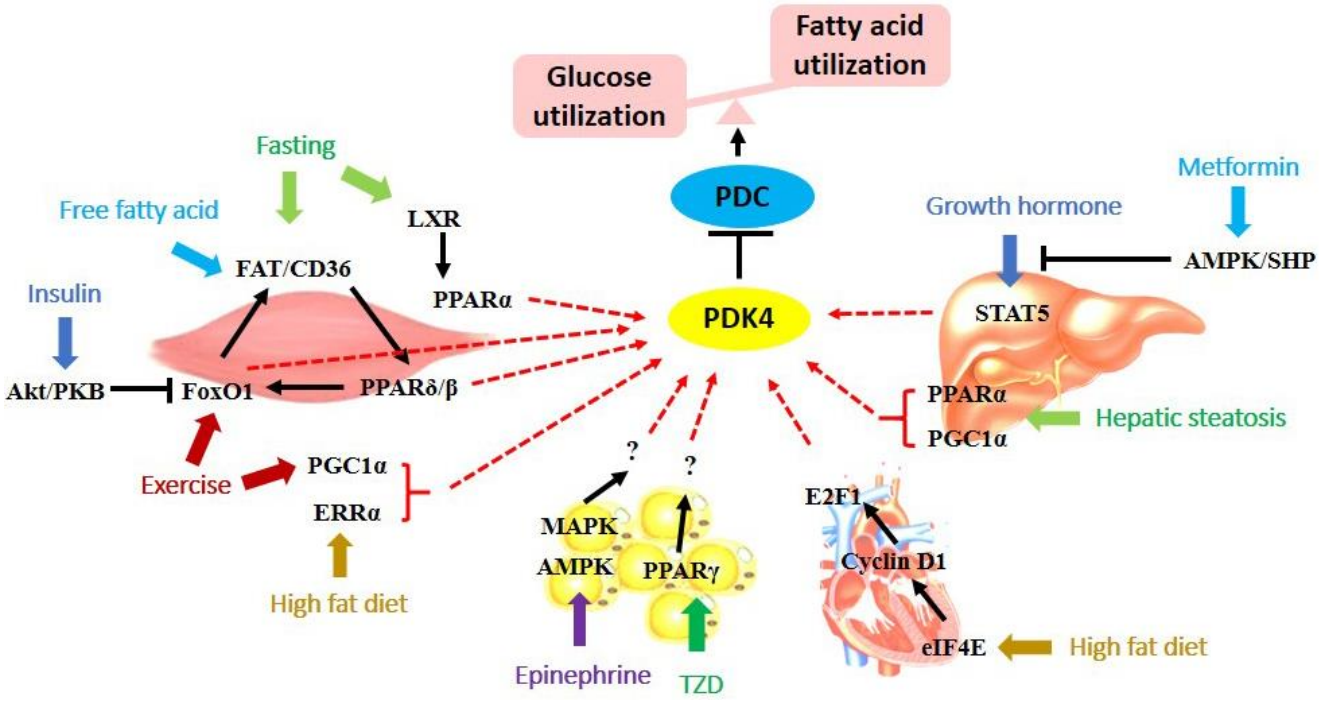

Figure 2.2 Schematic representation of the transcriptional regulation pathway of PDK4 in skeletal muscle, liver, white adipose tissue and heart under different nutritional states. Inactivation of PDC by up-regulation of PDK4 can switch glucose catabolism to fatty acid utilization. PDC: pyruvate dehydrogenase complex. PDK4: pyruvate dehydrogenase kinase 4. FoxO1: Forkhead box protein O1, forkhead homologue in rhabdomyosarcoma. LXR: liver X receptor. PPAR: peroxisome proliferator-activated receptor. ERRα: estrogen related receptor α. PGC1α: PPARγ co-activator 1α. AMPK/SHP: 5'-AMP-activated protein kinase/small heterodimer partner. MAPK: p38 mitogen-activated protein kinase. TZD: thiazolidinediones.

CHAPTER 3 Chickens Selected for High or Low Body Weight Differ in Fatty Acid Oxidation Efficiency and Metabolic Flexibility in Skeletal Muscle and Abdominal Fat

3.1 Abstract

Metabolic flexibility is the ability of a system to adjust fuel (glucose, fatty acids and amino acids) oxidation based on nutrient availability. The ability to alter substrate oxidation in response to nutritional state depends on the balance between oxidation and storage capacities. In starvation states, glucose is scarce and fatty acid oxidation is used to meet cellular energy requirements. The Virginia lines of chickens are a unique model of anorexia and obesity that have resulted from long-term (56 generations) divergent selection for high (HWS) or low (LWS) juvenile body weight, respectively. We hypothesized that hyperphagia and obesity in juvenile HWS chickens is associated with reduced fat oxidation efficiency and metabolic inflexibility in skeletal muscle and abdominal fat. In experiment 1, we collected hypothalamus, *Pectoralis major* and abdominal fat from 56-day old male HWS and LWS chickens (n=8) after 16h of fasting. Fatty acid oxidation was assessed by measuring and summing $^{14}CO_2$ production and ^{14}C-labeled acid-soluble metabolites (ASM) from the oxidation of [1-^{14}C] palmitic acid. The ratio of CO_2/ASM was calculated as a measurement of fatty acid oxidation efficiency. In abdominal fat, Citrate Synthase (CS) activity was measured. In Experimental 2, we compared the fatty acid oxidation capacity and efficiency of fast-twitch white skeletal muscle (*Pectoralis major*) and slow-twitch red skeletal muscle (gastrocnemius) in 61 day-old male HWS and LWS chickens (n=7) after a 16h fast as described above.

Metabolic flexibility was assessed by measuring the decrease in pyruvate oxidation in the presence of free fatty acids. Data were analyzed within each tissue by ANOVA using JMP 10.0 with genetic line (HWS and LWS) as the only effect in the statistical model. The rate of CO_2 production was greater in 56 day-old LWS chickens than in HWS chickens for both the abdominal fat ($P = 0.001$) and hypothalamus ($P = 0.003$). The rate of ASM production was greater ($P = 0.003$) in the abdominal fat of HWS than LWS chickens. Total palmitate oxidation, as a sum of CO_2 and ASM production, was greater ($P = 0.003$) in the abdominal fat of HWS chickens as compared to LWS. The ratio of CO_2/ASM production was greater ($P < 0.0001$) in the abdominal fat of LWS than HWS chickens. For the two skeletal muscle tissues, the difference was significant only for CO_2 production in gastrocnemius ($P = 0.02$), where LWS had a greater rate as compared to HWS. However, metabolic flexibility was greater ($P = 0.006$) in the *Pectoralis major* of LWS as compared to HWS chickens. Moreover, the LWS chickens had much greater ($P < 0.0001$) CS activity in abdominal fat as compared to HWS chickens. The results suggest that the LWS chickens have greater metabolic flexibility and fatty acid oxidation efficiency in skeletal muscle and abdominal fat compared to the HWS chickens.

3.2 Introduction

The regulation of energy balance in the animal involves a complex interplay between energy sensing in the brain and output of signals via neuronal effector pathways that affect energy intake and expenditure. The hypothalamus has an important role in integrating signals from visceral organs to control energy intake. However, mechanisms through which the hypothalamus senses the changes in energy balance and how organs such as skeletal muscle and white adipose tissue respond with altered metabolic activities is unclear.

In the present study, we used 56- and 61-day-old Virginia lines of chickens that have resulted from long-term (56 generations) divergent selection for high (HWS) or low (LWS) juvenile (56-day-old) body weight. Selection for body weight, with a more than tenfold difference in body weight now observed between the lines at selection age, led to correlated responses in body composition. HWS and LWS chickens respond with differential food intake to exogenous orexigenic and anorexigenic neuropeptides, and these differences are associated with changes in hypothalamic chemistry (Hagen et al., 2013; Newmyer et al., 2013). Lipid oxidation has been proposed as an energy sensing mechanism in hypothalamus. As signals of nutrient abundance, lipids are able to modulate feeding in hypothalamus (Lopez and Vidal-Puig, 2008). Because of differences in feeding behavior and body composition between the lines, fatty acid oxidation and metabolic flexibility might provide a link between energy intake and expenditure. We hypothesized that hyperphagia and obesity in juvenile HWS chickens are associated with reduced fat oxidation efficiency and metabolic inflexibility in skeletal muscle and abdominal fat.

3.3 Materials and Methods

3.3.1 Animals

Animal handling and care were performed according to the National Research Council publication, Guide for Care and Use of Laboratory Animals. All protocols were approved by the Institutional Animal Care and Use Committee at Virginia Tech. The HWS and LWS chickens were established from a common founder population generated by crosses among seven inbred lines of White Plymouth Rock chickens (Dunnington and Siegel, 1996; Dunnington et al., 2013). The lines have been maintained as closed populations by continuous selection for high or low body weight at 56 days of age. Description of the breeding and maintenance of the populations is published elsewhere (Dunnington and Siegel, 1996; Marquez et al., 2010; Dunnington et al., 2013). For the present experiments, feed and water were supplied *ad libitum*. The diet fed was the same as that which was fed throughout the selection experiment and consisted of 20% crude protein and 2,685 kcal metabolizable energy/kg in mash form. Animals were fasted for 16 hours prior to sample collection in all experiments.

3.3.2 Fatty acid oxidation and citrate synthase activity assays

At 56 days of age, 8 randomly selected male chickens from each line were euthanized by cervical dislocation for collection of *Pectoralis major*, abdominal fat and hypothalamus. At 61 days of age, *Pectoralis major* and gastrocnemius were collected from another 14 randomly selected male chickens (7 for each line) for fatty acid oxidation assays. The hypothalamus was dissected visually based on the following anatomical landmarks: anterior cut made at the corticoseptomesencephalic tract, posterior

cut at the third cranial nerves, laterally cut 2 mm parallel to the midline on both sides of the brain and finally the dorsal cut from the anterior commissure to 1.0 mm ventral to the posterior commissure (Puelles, 2007).

The tissue samples were diluted 1:20 (weight:volume) in a buffer containing 0.25 M sucrose, 1 mM EDTA, 0.01 M Tris-Cl and 2 mM ATP, pH 7.4. The sample was then minced 200 times with mincing scissors and transferred to a 2 mL glass homogenizing tube. The sample was then homogenized on ice with a Polytron homogenizer with a Teflon glass pestle for 30 sec at 300 RPM. This was repeated in 30 sec pulses alternating with 30 sec on ice 12 times. The homogenate was then transferred to a microcentrifuge tube.

Fatty acid oxidation was assessed by measuring and summing $^{14}CO_2$ production and ^{14}C-labeled acid-soluble metabolites from the oxidation of [1-^{14}C] palmitic acid (Perkin-Elmer, Waltham, MA) as previously described (Frisard et al., 2010).

Citrate synthase (CS) activity was measured only in abdominal fat, the tissue that showed the most differences in fatty acid oxidation between HWS and LWS. CS catalyzes the formation of citrate and CoASH from acetyl-CoA and oxaloacetate and CoASH reduces 5,5'-Dithiobis-2-Nitrobenzoic Acid (DTNB) levels. CS activity was determined from the reduction of DTNB over time. 10 mL of 1:5 diluted tissue homogenate was added in duplicate to 170 µL solution containing Tris buffer (0.1 M, pH 8.3), DTNB (1 mM, in 0.1 M Tris buffer) and oxaloacetate (0.01 M, in 0.1 M Tris buffer). Following a 2 min background reading, the spectrophotometer (SPECTRAmax ME, Molecular Devices Corporation, Sunnyvale California) was calibrated and 30 µL of 3 mM acetyl CoA was added to initiate the reaction. Absorbance was measured at 405 nm

at 37 ℃ every 12 sec for 7 min. Maximum CS activity was calculated and reported as nmol · mg^{-1} · min^{-1}.

3.3.3 Metabolic flexibility in different skeletal muscle fiber sub-types

For PDH activity and metabolic flexibility assays in different skeletal muscle tissues, 7 LWS and 7 HWS randomly selected male chickens were fasted as described in the animals section and on day 61 euthanized by cervical dislocation and sampled for *Pectoralis major* and gastrocnemius muscle. Tissues were collected and processed as described above.

Pyruvate oxidation was assessed by measuring $^{14}CO_2$ production from the oxidation of [1-^{14}C] pyruvate (Perkin-Elmer, Waltham, MA) as previously described (Power et al., 2007; Anderson et al., 2013). Metabolic flexibility was assessed by measuring [1-^{14}C] pyruvate oxidation ± non-labeled BSA (0.5%) bound-palmitic acid. Flexibility is denoted by the percentage decrease in pyruvate oxidation in the presence of free fatty acid (e.g. a higher percentage is indicative of greater metabolic flexibility).

3.3.4 Statistical analysis

Fatty acid oxidation, PDH and CS activity and metabolic flexibility data were analyzed within each tissue, with genetic line (HWS or LWS) as the only effect. For all analyses, data normality and heterogeneity of variances were evaluated then ANOVA performed using JMP Pro version 10.0 (SAS Institute, USA) and the Fit Model platform. Data are presented as least square means ± SEM and statistical significance assigned at $P < 0.05$.

3.4 Results

3.4.1 Fatty acid oxidation efficiency in skeletal muscle, abdominal fat and hypothalamus

Complete oxidation of [1-^{14}C] palmitic acid leads to the formation of $^{14}CO_2$, while incomplete oxidation of [1-^{14}C] palmitic acid represents metabolic byproducts of fat oxidation that may have escaped β-oxidation or the TCA cycle. Fatty acid oxidation yields acetyl CoA, which can then feed into the TCA cycle, yielding CO_2 as a byproduct. When substrate flux through the β-oxidation pathway outpaces the activity of the TCA cycle, rates of incomplete oxidation increase, resulting in a corresponding rise in acylcarnitine production and accumulation. Acylcarnitine metabolites might reflect a state of mitochondrial stress that, in turn, disrupts glucose tolerance. However, higher acid soluble metabolites (ASM) production is only seen as a detriment when not accompanied by likewise higher CO_2 production, thus in the present study, the fatty acid oxidation data were also expressed as the ratio of CO_2/ASM as a measure of β oxidative efficiency. Disruptions in this ratio may represent mitochondrial overload and signal an environment that may be toxic to insulin signaling.

The rate of CO_2 production from palmitate oxidation was greater in 56 day-old LWS chickens than in HWS chickens for both the abdominal fat (P = 0.001) and hypothalamus (P = 0.003) (Figure 3.1). The rate of ASM production was greater (P = 0.003) in the abdominal fat of HWS than LWS chickens (Figure 3.2). Total palmitate oxidation, as a sum of CO_2 and ASM production, was greater (P = 0.003) in the abdominal fat of HWS chickens as compared to LWS (Figure 3.3). The ratio of CO_2/ASM production, a measure of fatty acid oxidation efficiency, was greater (P < 0.0001) in the abdominal fat of LWS than HWS chickens (Figure 3.4). There were no

differences observed in fatty acid oxidation between the HWS and LWS in *Pectoralis major*.

3.4.2 Fatty acid oxidation and metabolic flexibility in gastrocnemius and *Pectoralis major*

We next compared the fatty acid oxidation capacity and efficiency of fast-twitch white skeletal muscle (*Pectoralis major*) and slow-twitch red skeletal muscle (gastrocnemius) in 61 day-old HWS and LWS. The two tissues were different in fatty acid oxidation. While rates of CO_2 ($P = 0.02$, Figure 3.5), ASM production ($P = 0.2$, Figure 3.6), total palmitate oxidation ($P = 0.1$, Figure 3.7) and fatty acid oxidation efficiency ($P = 0.07$, Figure 3.8) were all greater in the gastrocnemius of LWS as compared to HWS, the difference was significant only for CO_2 production. In the *Pectoralis major*, there were no significant differences in fatty acid oxidation between the lines.

While PDH activity did not differ between 61 day-old HWS and LWS in either of the skeletal muscle tissues (Figure 3.9), metabolic flexibility (percent change in PDH activity in response to treatment with free fatty acids) was greater ($P = 0.006$) in the *Pectoralis major* of LWS as compared to HWS chickens (Figure 3.10). The LWS chickens also had much greater ($P < 0.0001$) citrate synthase activity in abdominal fat as compared to HWS chickens (130 ± 9 vs. 60 ± 5 nmol $\cdot$ mg^{-1} $\cdot$ min^{-1}, respectively).

3.5 Discussion

It has been suggested that hypothalamic neurons are able to oxidize fatty acids and that alterations in this process are associated with appetite dysregulation, although

there have been findings to contradict this theory (Lopaschuk et al., 2010). In the hypothalamus, we observed greater rates of CO_2 production from palmitate oxidation in the LWS chickens, indicative of greater energy production and total oxidation, with no significant differences in ASM production, palmitate oxidation or fatty acid oxidation efficiency, indicating the disruption of the fuel sensing status in LWS. Other studies have shown that long-chain fatty acids (LCFA) serve as signals in modulating energy balance, although the role of fatty acid oxidation in signaling is unclear (Lopez and Vidal-Puig, 2008; Serra et al., 2013). Carnitine palmitoyl-coenzyme A transferase-1 (CPT1) is a rate-limiting step in the oxidation of fatty acids, because it is an enzyme that controls the transport of LCFA into the mitochondria, where they undergo β-oxidation (Serra et al., 2013). The activity of CPT is likely to influence the available pool of LCFA and ensuing rates of oxidation. While three CPT paralogs have been identified in mammals (a, b and c), only two have been identified in chickens (a and b) and *CPT1b* was revealed to be a differentially-expressed gene in the hypothalamus of HWS and LWS (Ka et al., 2013). At 56 days of age, the abundance of *CPT1b* mRNA was greater in skeletal muscle (*Pectoralis major*) than liver, adipose or brain, and expression was greater in the hypothalamus of HWS than LWS, whereas in skeletal muscle, there was greater expression in LWS compared to HWS (Ka et al., 2013). However, in mitochondrial extracts from hypothalamus, abundance of CPT1b protein was only different between female HWS and LWS, with greater expression in the LWS (Ka et al., 2013). Malonyl CoA is a negative feedback inhibitor of CPT1 activity, and AMP-activated protein kinase regulates malonyl CoA concentrations through regulation of acetyl-CoA carboxylase.

There are differential responses of the lines in feeding behavior after stimulation or inhibition of AMPK (Xu et al., 2011).

The LWS chickens showed greater fatty acid oxidation efficiency in abdominal fat and slow-twitch red muscle fiber sub-types in the fasting state. In fast-twitch white muscle, there was no significant difference. This suggests that red muscle, which contains more mitochondria as compared to white muscle, is a site of enhanced fatty acid oxidation in the LWS chickens. In chickens, the *Pectoralis major* is composed exclusively of type II, fast-twitch, white muscle fibers, whereas the gastrocnemius is composed mainly of type I, slow-twitch red muscle fiber sub-types (Ashmore and Doerr, 1971).

Calabotta et al.(Calabotta et al., 1985) reported enhanced rates of lipolysis and lipogenesis in abdominal fat of 28-day old LWS chickens as compared to their HWS counterparts. They suggested that the greater rate of lipolysis prevented net fat accumulation in the LWS chickens, although the mechanism underlying the differences in rate of metabolism were unknown. Those data combined with the present results suggest a greater availability of fatty acids for oxidation that are accompanied by greater rates of oxidation and oxidative efficiency in LWS chickens.

As a pace-making enzyme in the first step of the TCA Cycle, citrate synthase (CS) can regulate entry of acetyl-CoA into the TCA cycle. It is also a widely used quantitative marker for mitochondrial content (Larsen et al., 2012). In 56-day-old LWS chickens there was more than two-fold greater CS activity. These results are consistent with the fatty acid oxidation data, that the abdominal fat of LWS are more densely populated by mitochondria, and associated with greater rates of CO_2 production. This corresponded to

reduced rates of ASM production, indicating that the output of the TCA cycle is more closely matched to the rates of fatty acid oxidation, associated with enhanced oxidative efficiency in the LWS.

The metabolism of fatty acids and glucose are coordinately regulated such that the cell can adapt fuel oxidation to the nutrient availability (relative abundance of glucose vs. fatty acids). In the starved state, free fatty acids released from adipose tissue are selectively used for oxidative ATP generation in peripheral tissues and liver, and hepatic gluconeogenesis maintains plasma glucose homeostasis (Jeong et al., 2012). This process is regulated by PDC. The LWS chickens showed much greater metabolic flexibility (down-regulating pyruvate dehydrogenase to accommodate the influx of acetyl CoA from fatty acid oxidation) in response to treatment with palmitate in both adipose tissue and skeletal muscle. This can be due to the increased activity of PDC, which regulates the entry of glycolytic products into the tri-carboxylic acid cycle by catalyzing the oxidative decarboxylation of pyruvate to acetyl-CoA in mitochondria.

In summary, these data clearly demonstrated differences in oxidative metabolism between HWS and LWS in hypothalamus, skeletal muscle and adipose tissue. The molecular mechanism underlying these differences was unclear, but as described in the next chapter, may be associated with differences in expression of metabolic flexibility-associated genes.

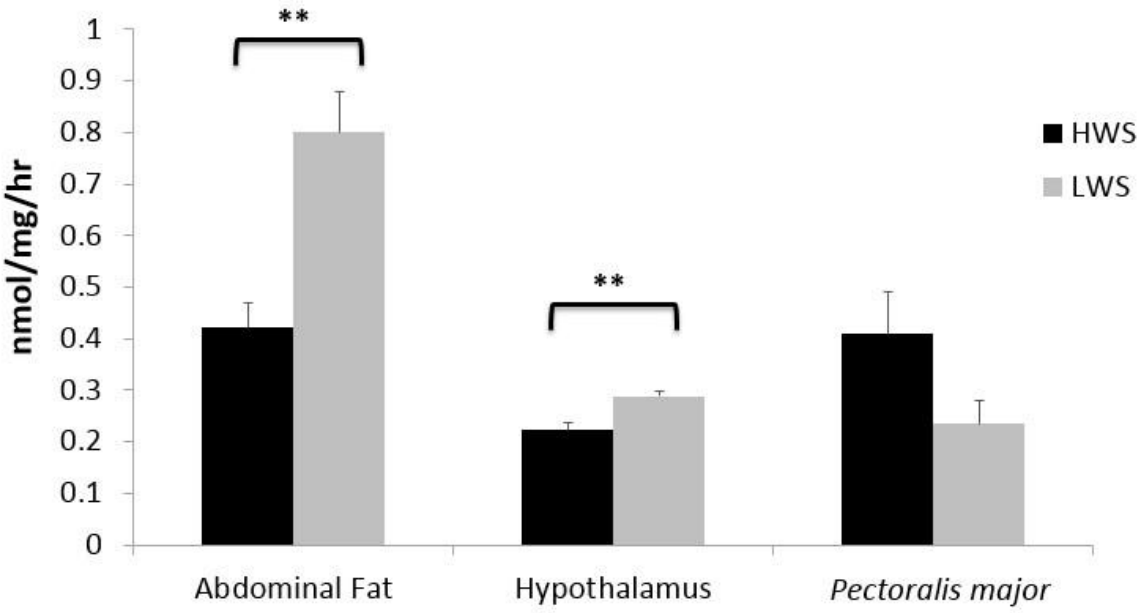

Figure 3.1 CO_2 production from fatty acid oxidation in abdominal fat, hypothalamus and *Pectoralis major* of 56-day-old male HWS and LWS chickens. n=8. $^{**}P < 0.01$. Values represent least squares means ± SEM.

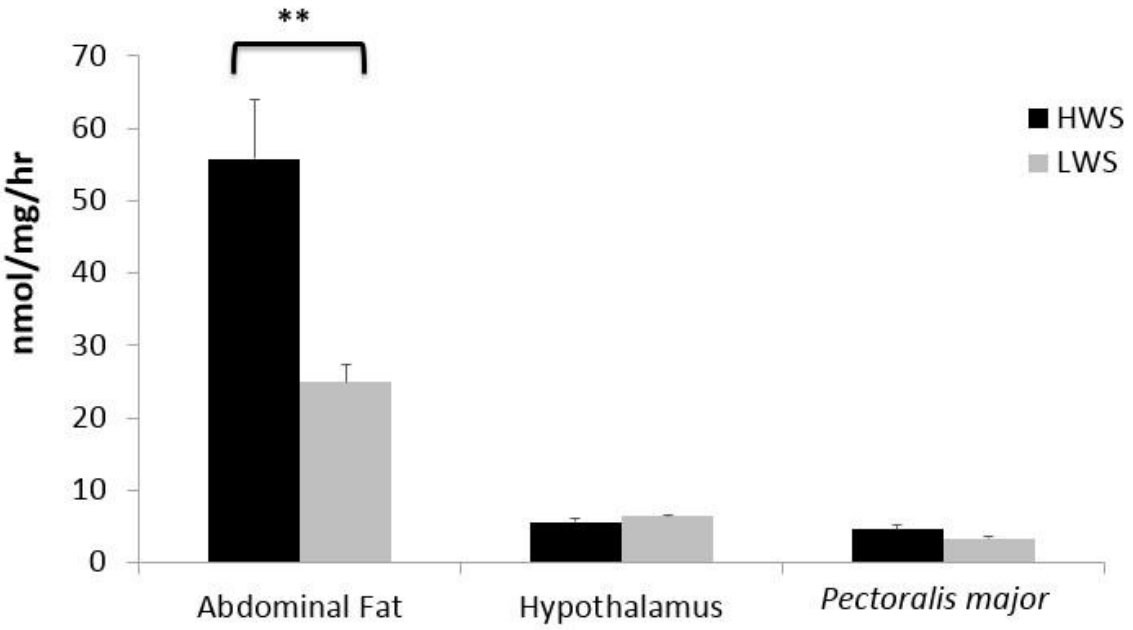

Figure 3.2 Acid soluble metabolites (ASM) from fatty acid oxidation in abdominal fat, hypothalamus and *Pectoralis major* of 56-day-old male HWS and LWS chickens. n=8. $^{**}P < 0.01$. Values represent least squares means ± SEM.

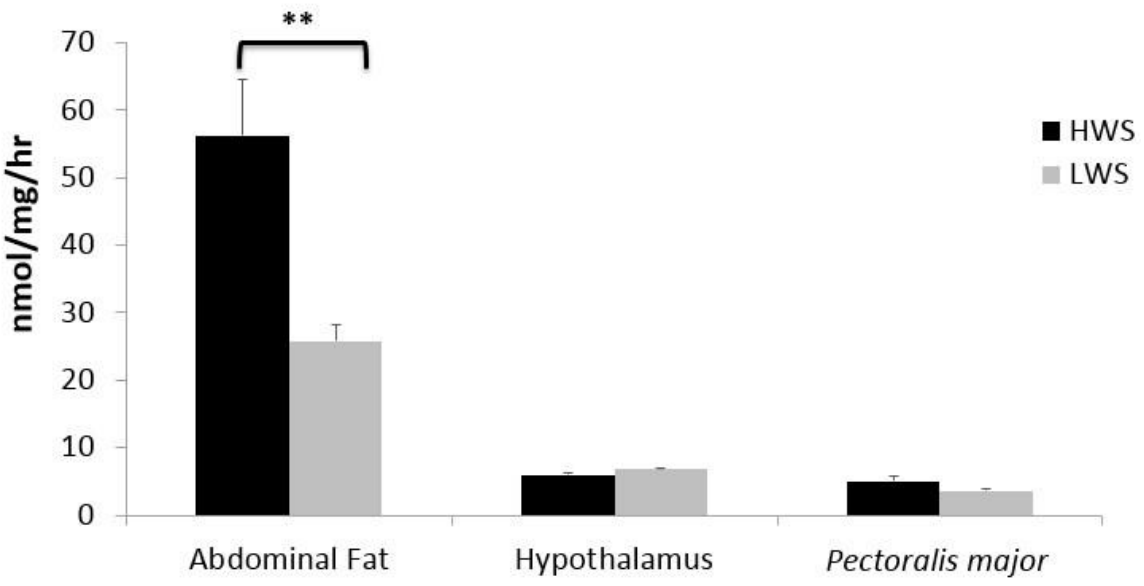

Figure 3.3 Total palmitate oxidation (CO_2 production + ASM production) from fatty acid oxidation in abdominal fat, hypothalamus and *Pectoralis major* of 56-day-old male HWS and LWS chickens. n=8. $^{**}P < 0.01$. Values represent least squares means ± SEM.

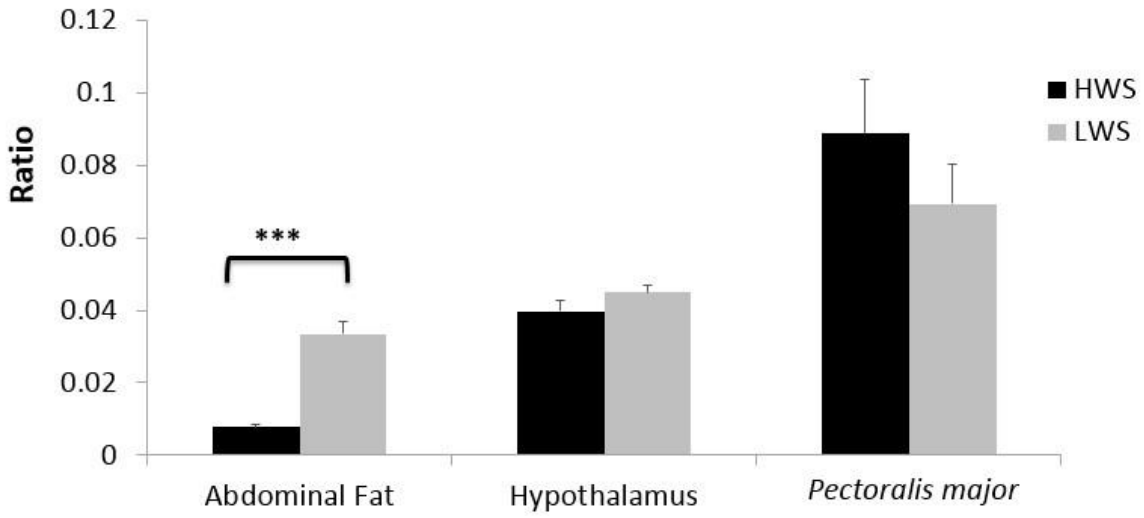

Figure 3.4 CO_2/ASM ratio from fatty acid oxidation in abdominal fat, hypothalamus and *Pectoralis major* of 56-day-old male HWS and LWS chickens. n=8. ***$P < 0.001$. Values represent least squares means ± SEM.

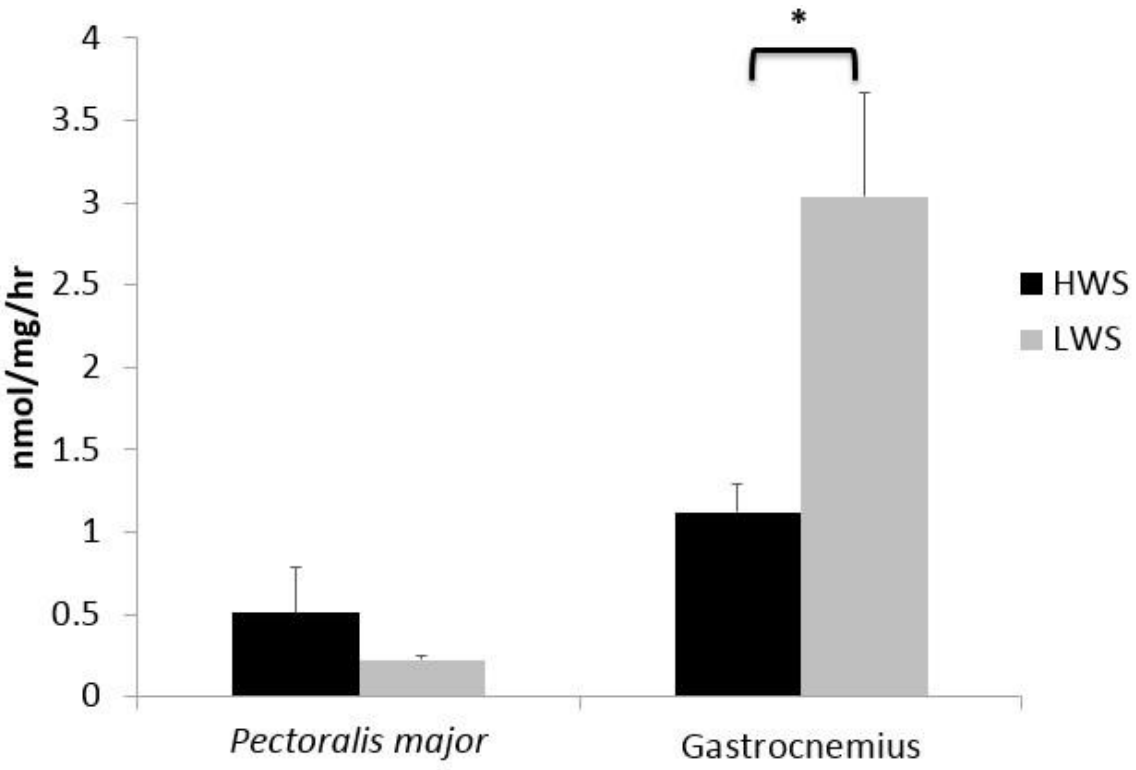

Figure 3.5 CO_2 production from fatty acid oxidation in *Pectoralis major* and gastrocnemius of 61-day-old male HWS and LWS chickens. n=7. *$P < 0.05$. Values represent least squares means ± SEM.

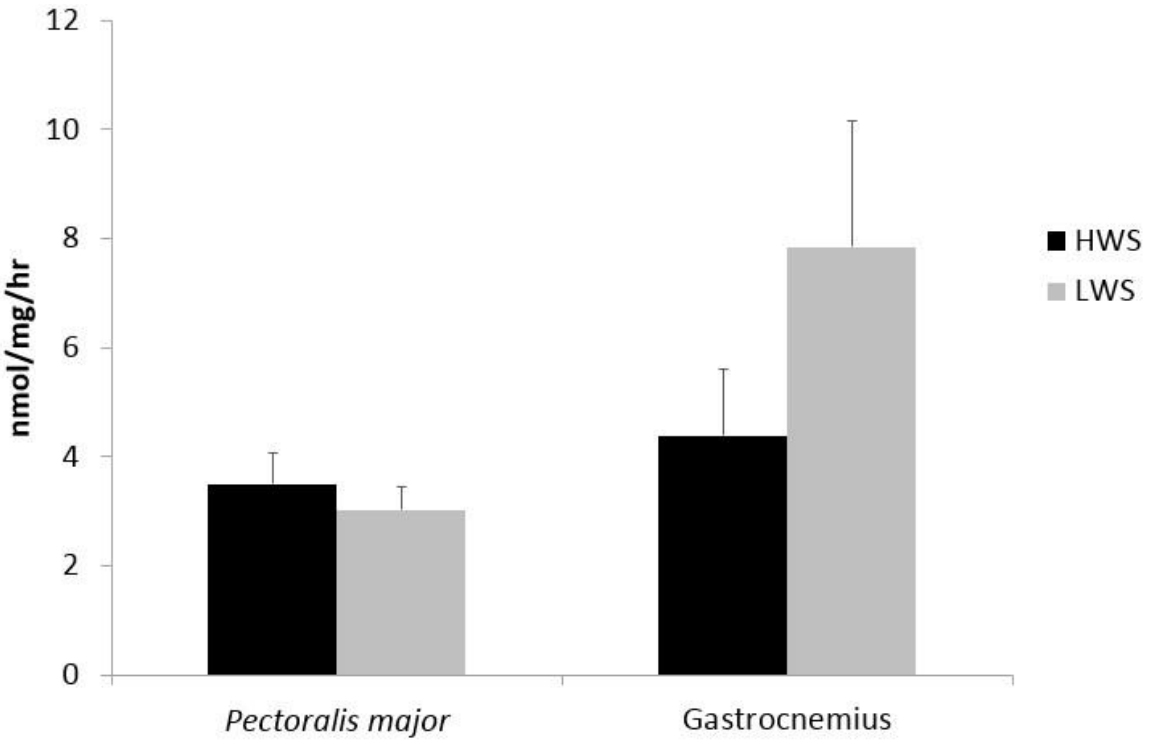

Figure 3.6 Acid soluble metabolites (ASM) production from fatty acid oxidation in *Pectoralis major* and gastrocnemius of 61-day-old male HWS and LWS chickens. n=7. Values represent least squares means ± SEM.

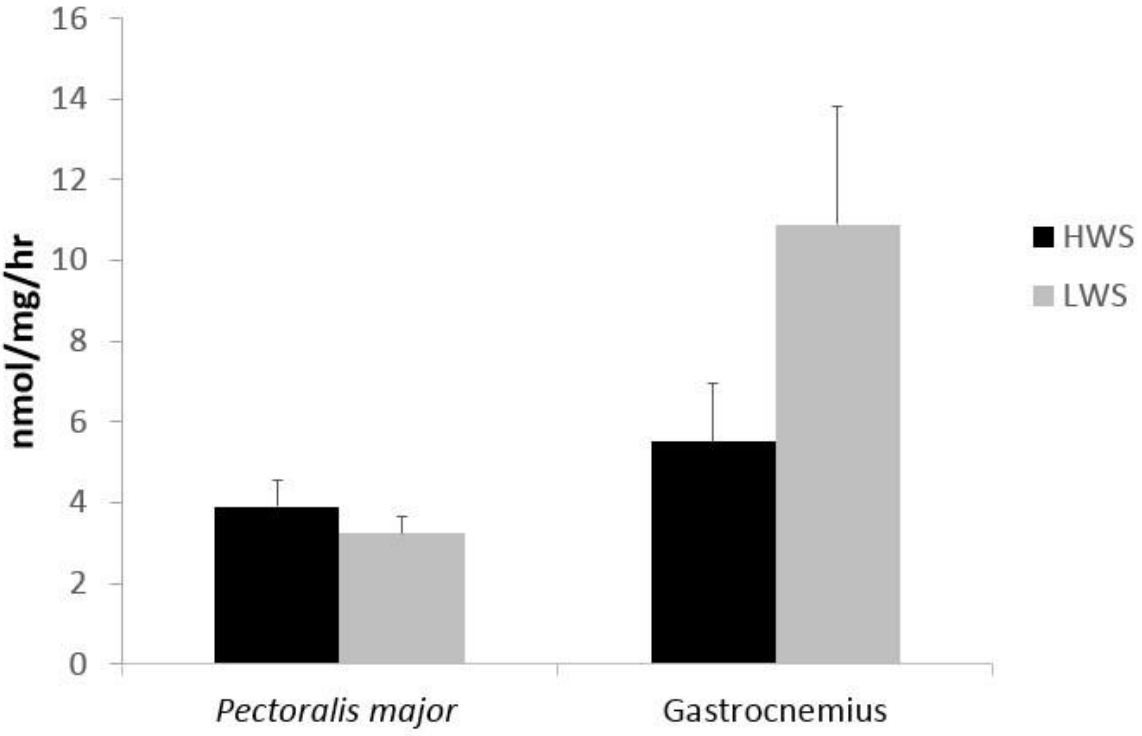

Figure 3.7 Total palmitate oxidation (CO_2 production + ASM production) from fatty acid oxidation in *Pectoralis major* and gastrocnemius of 61-day-old male HWS and LWS chickens. n=7. Values represent least squares means ± SEM.

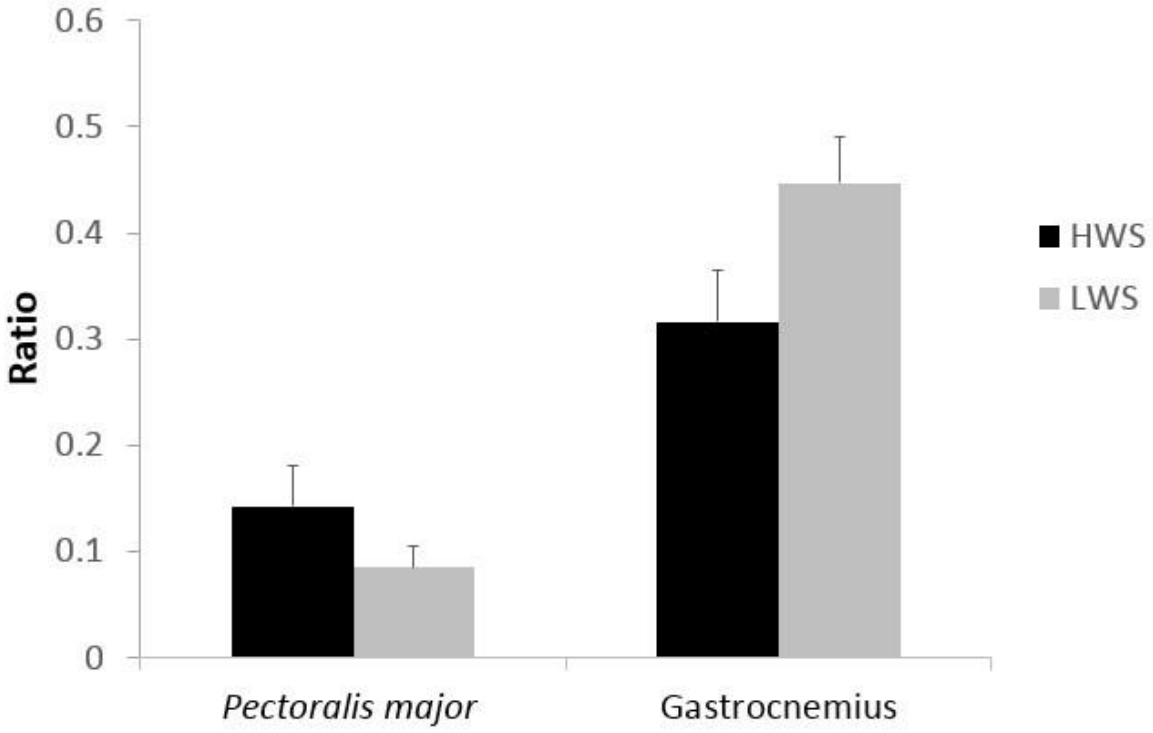

Figure 3.8 CO_2/ASM ratio from fatty acid oxidation in *Pectoralis major* and gastrocnemius of 61-day-old male HWS and LWS chickens. n=7. Values represent least squares means ± SEM.

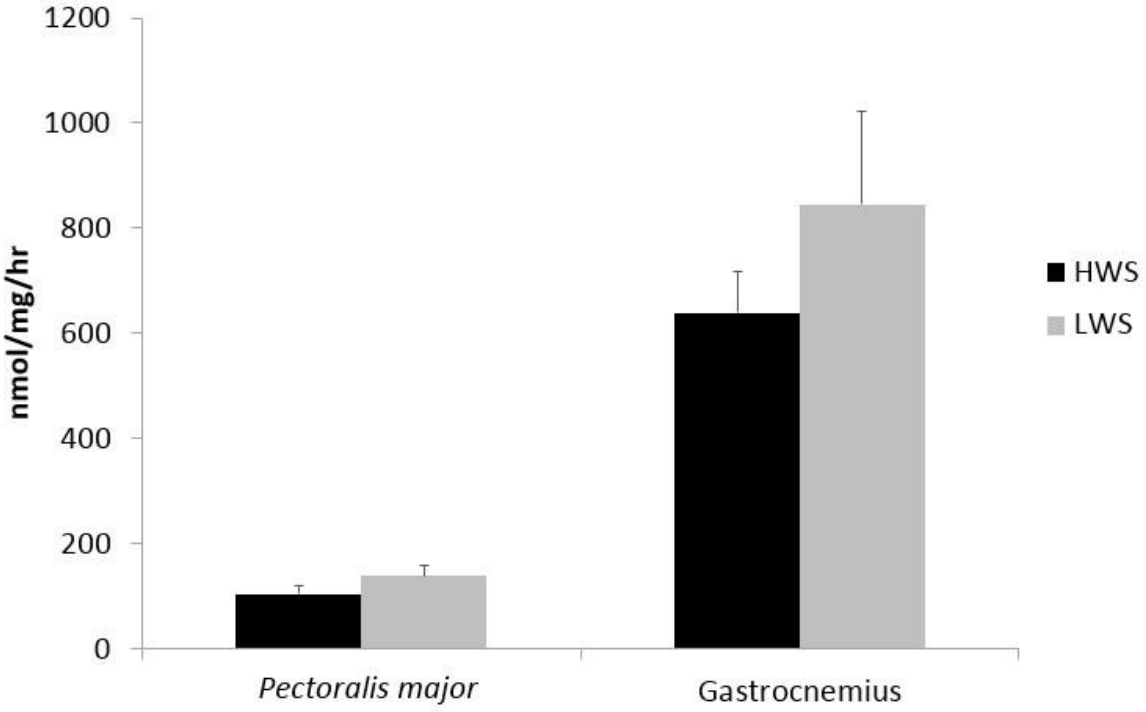

Figure 3.9 Pyruvate dehydrogenase (PDH) activity in *Pectoralis major* and gastrocnemius skeletal muscle tissues of 61-day-old male HWS and LWS chickens. n=7. Values represent least squares means ± SEM.

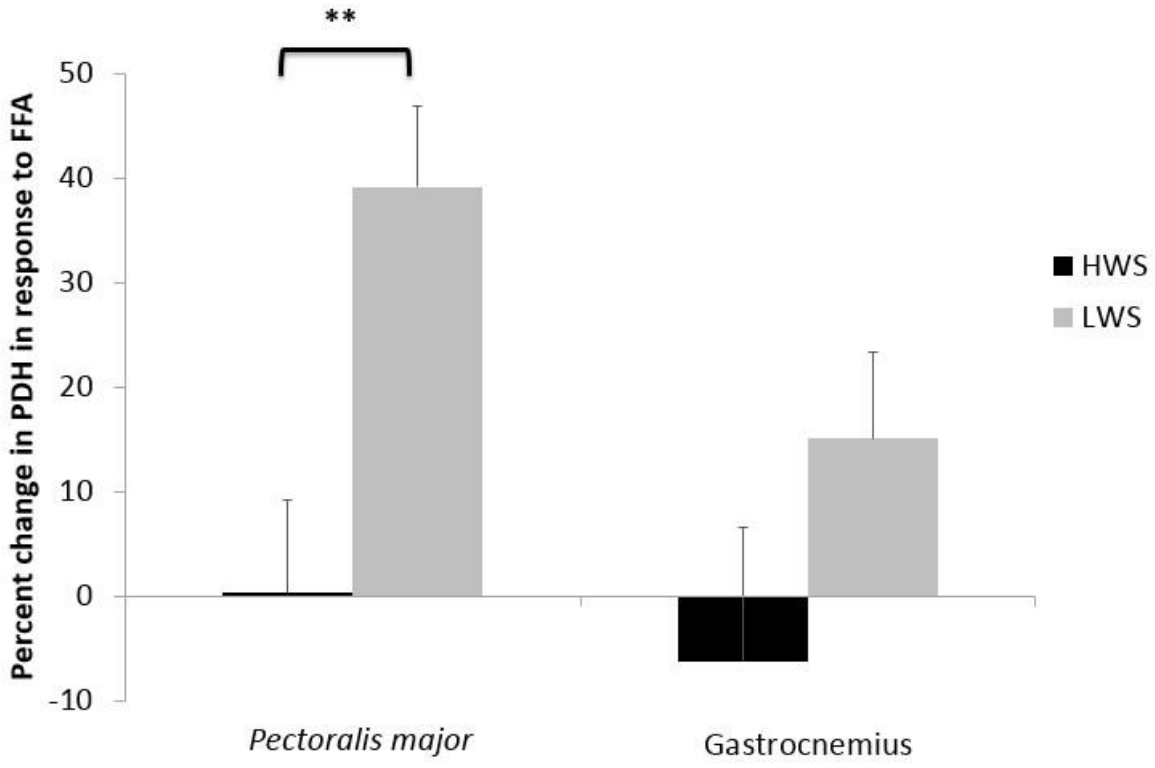

Figure 3.10 Metabolic flexibility, which was measured as the percent change in PDH activity in response to free fatty acids, in *Pectoralis major* and gastrocnemius skeletal muscle tissues of 61-day-old male HWS and LWS chickens. n=7. $^{**}P < 0.01$. Values represent least squares means ± SEM.

CHAPTER 4 Chickens Selected for High or Low Body Weight Differ in Expression of Metabolic Flexibility-Related Genes in Skeletal Muscle and White Adipose Tissue

4.1 Abstract

The Virginia lines of chickens are a unique model of anorexia and obesity that have resulted from 56 generations of selection for high (HWS) or low (LWS) body weight. We hypothesized that the differences observed in fatty acid oxidation efficiency and metabolic efficiency are associated with differences in expression of metabolic flexibility-related genes. We collected hypothalamus, liver, pectoralis major, gastrocnemius, abdominal fat, clavicular fat and subcutaneous fat from 28- and 56-day old HWS and LWS chickens (n=10, 5 males and females). The mRNA abundance of pyruvate dehydrogenase kinase 4 (*PDK4*), forkhead box O1 (*FoxO1*), peroxisome proliferator-activated receptor γ (*PPARγ*) and *PPARγ* co-activator α (*PGC1α*) was measured by real-time PCR. Expression was calculated using the $\Delta\Delta C_T$ method, and analyzed within each tissue by ANOVA using JMP 10.0. The statistical model included the main effects of sex, genetic line, age and the interactions between them. Means were separated using Tukey's Test. In 56-day old chickens, there was greater ($P < 0.05$) *PDK4* mRNA in HWS than LWS in pectoralis major, gastrocnemius, abdominal fat and subcutaneous fat, and lower ($P = 0.02$) *PDK4* abundance in clavicular fat, irrespective of age. There was an interaction of sex by line ($P = 0.002$) on *PDK4* mRNA in hypothalamus, where there was greatest expression in HWS females. Abundance of *FoxO1* showed a similar pattern as *PDK4*, where HWS chickens had greater *FoxO1* mRNA than LWS in the two skeletal muscles ($P < 0.01$) and at 56 days in subcutaneous

fat ($P = 0.02$). In both clavicular fat and hypothalamus, there was an age x sex x line interaction, where *FoxO1* mRNA was greatest in LWS males at 28 and 56 days of age. Expression of *PPARγ* mRNA was greater ($P < 0.05$) in LWS than HWS in clavicular fat and subcutaneous fat at both ages, and at 28 days in the skeletal muscles. For *PGC1α*, in gastrocnemius there was greatest expression in HWS males ($P = 0.03$). The results suggest that the LWS chickens have greater metabolic flexibility and fatty acid oxidation efficiency due to down-regulation of pyruvate dehydrogenase to accommodate the influx of acetyl CoA from fatty acid oxidation in skeletal muscle and white adipose tissue. There appears to be coordinate regulation of *PDK4* and *FoxO1* mRNA. These data suggest that these could be metabolic differences between different fat depots and that transcription factors regulating the PDKs are differentially regulated in HWS and LWS.

4.2 Introduction

The pyruvate dehydrogenase complex (PDC) is rendered inactive by phosphorylation of the α-subunit of its pyruvate dehydrogenase component by pyruvate dehydrogenase kinase (PDK) (Kwon and Harris, 2004). Mammalian PDK has been shown to exist in several isoforms (PDK1-PDK4) that are highly expressed in muscle tissues and liver (Gudi et al., 1995). The expression of *PDK4* is a major determinant of PDK activity (Strumilo, 2005). Fasting, diabetes, and high-fat diet feeding are all associated with increased expression of *PDK4* and total PDK activity in rat skeletal muscle (Wu et al., 1999; Holness et al., 2000). *PDK4* expression is also positively correlated with PDK activity in rat adipose tissue and human adipocytes (Cadoudal et al., 2008) and is regulated by several transcription factors, such as members of the FoxO and PPAR families (Constantin-Teodosiu et al., 2012).

As one of the forkhead-type transcription factors, FoxO1 (forkhead box O1) is activated downstream of the insulin signaling pathway via phosphoinositide 3-kinase (PI3K), which is involved in cellular proliferation and energy metabolism (Guarente and Kenyon, 2000). In skeletal muscle, which contributes to more than 30% of resting metabolic rate and 80% of whole body glucose uptake, *FoxO1* is responsible for switching from oxidation of carbohydrates as the major energy source to fatty acids in the fasting state (Gross et al., 2008). There is evidence showing that levels of *PDK4* mRNA are up-regulated through the direct binding of FoxO1 to the promoter region of *PDK4* in C2C12 mouse myoblast cells during energy deprivation (Furuyama et al., 2003).

Peroxisome proliferator-activated receptor gamma (PPARγ) is a nuclear receptor that can be activated by thiazolidinediones (TZD) (Wan et al., 2012) and endogenous

ligands, such as free fatty acids. The PPARγ can regulate the expression of more than 10 genes in mammals, including *PDK4* (Sears et al., 2007). It was observed that epinephrine-mediated increases in *PDK4* mRNA in human white adipose tissue were mediated via PPARγ (Wan et al., 2010). As a transcriptional coactivator of PPARγ, peroxisome proliferator-activated receptor γ coactivator α (PGC1α) acts as a key regulator of cellular energy metabolism (Puigserver and Spiegelman, 2003) and can enhance the T_3-mediated induction of *PDK4* mRNA in rats (Attia et al., 2010). It can also down-regulate glucose oxidation while activating mitochondrial fatty acid oxidation in skeletal muscle tissues of rodents (Lin, 2009; Holloway et al., 2010). PGC1α can also augment the transcriptional function of *FoxO1* in liver to regulate gluconeogenic genes (Gross et al., 2008). Other *PPAR* family members, *PPAR*α and *PPAR*β/δ, glucocorticoid receptor (*GR*), Thyroid hormone receptors (*TR*s), adiponectin and *AMPK* are all reported to participate in *PDK4* modulation (Wende et al., 2005; Araki and Motojima, 2006; Connaughton et al., 2010; Song et al., 2010; Jeong et al., 2012).

In the present study, we investigated gene expression in different tissues of the 28- and 56-day-old Virginia lines of chickens that have resulted from long-term (56 generations) divergent selection for high (HWS) or low (LWS) juvenile (56-day-old) body weight. Selection for body weight, with a more than tenfold difference in body weight now observed between the lines at selection age, led to correlated responses in body composition. We hypothesized that the enhanced fatty acid oxidation and metabolic flexibility in LWS are associated with differences in expression of metabolic flexibility-related genes (*PDK4*, *FoxO1*, *PPARγ* and *PGC1α*).

4.3 Materials and Methods

4.3.1 Animals

The details about the animals used in this study are the same as described in 3.3.1.

4.3.2 Real time PCR assays

For measuring mRNA abundance of metabolic-associated factors, 5 male and 5 female chickens randomly selected from HWS and LWS were euthanized by cervical dislocation on days 28 and 56 post-hatch. The hypothalamus, liver, *Pectoralis major*, gastrocnemius, abdominal fat, clavicular fat (fat above the clavicle) and subcutaneous fat were collected, snap-frozen in liquid nitrogen and transferred to -80°C.

Approximately 300 mg of the adipose tissue samples or 100 mg of other tissues from each chicken were added to a tube containing a 5 mm stainless steel bead (Qiagen) and 1 mL of Isol Lysis reagent (5-Prime, USA) and homogenized 2 x 2 min at 20 Hz with a Tissue Lyser II (Qiagen, USA). After incubation and centrifugation for 10 min for 12,000 x g at 4°C, the supernatant was removed and total RNA separated, following the manufacturer's instructions (5-Prime). Following the step of addition to 70% ethanol, mixtures were transferred to spin columns and total RNA purified using the RNeasy Mini Kit (Qiagen, USA), including the optional on-column RNase-free DNase I step (Qiagen, USA). The eluted total RNA samples were evaluated for integrity by agarose-formaldehyde gel electrophoresis and concentration and purity assessed by spectrophotometry at 260/280/230 nm with a Nanophotometer^{TM} Pearl (IMPLEN, USA).

Single-strand cDNA was synthesized from 200 ng total RNA in 20 µL reactions with a High Capacity cDNA Reverse Transcription Kit (Applied Biosystems, USA), following the manufacturer's instructions. Reactions were performed under the following

conditions: 25°C for 10 min, 37°C for 120 min, and 85°C for 5 min. Primers for real time PCR were designed with Primer Express 3.0 software (Applied Biosystems, USA) (Table 4.1) and amplification efficiency was validated for all primer pairs before use (95-100% efficiency). Real-time PCR was performed in duplicate in 10 µL volume reactions that contained 5 µL Fast SYBR Green Master Mix (Applied Biosystems, USA) and 3 µL of 10-fold diluted cDNA using a 7500 Fast Real-Time PCR System (Applied Biosystems, USA). PCR was performed under the following conditions: 95°C for 20 sec and 40 cycles of 90°C for 3 sec plus 60°C for 30 sec. A dissociation step consisting of 95°C for 15 sec, 60°C for 1 min, 95°C for 15 sec and 60°C for 15 sec was performed at the end of each PCR reaction to ensure amplicon specificity.

4.3.3 Statistical analysis

Real time PCR data were analyzed using the $\Delta\Delta C_T$ method, where β actin served as the endogenous control and day 28 HWS liver served as the calibrator sample. Relative quantities, calculated as $2^{-\Delta\Delta CT}$, were used for statistical analysis. ΔC_T represents the difference between C_T (the threshold cycle) values of the targeted gene and C_T values of the endogenous control gene. $\Delta\Delta C_T$ represents the difference between C_T values of the targeted sample and C_T values of the calibrator sample (Livak and Schmittgen, 2001). Real time PCR data were analyzed within each tissue, and the statistical model included the main effects of sex (male or female), genetic line (HWS or LWS), age (28 or 56 days) and the interactions between them. For all analyses, data normality and heterogeneity of variances were evaluated then ANOVA performed using JMP Pro version 10.0 (SAS Institute, USA) and the Fit Model platform. Means were separated using Tukey's Test.

Data are presented as least square means ± SEM and statistical significance assigned at $P < 0.05$.

4.4 Results

4.4.1 *PDK4* mRNA abundance in different tissues

We measured the relative abundance of *PDK4* mRNA in *Pectoralis major*, gastrocnemius, abdominal fat, clavicular fat, subcutaneous fat, hypothalamus and liver from the two lines after 16 hours of fasting at days 28 and 56 (Table 4.2-Table 4.8). For brevity, within each tissue, only the highest order significant effects in the statistical model involving genetic line are depicted graphically. There were no significant differences in the liver. The *Pectoralis major* (Figure 4.1), gastrocnemius (Figure 4.2), abdominal fat (Figure 4.3) and subcutaneous fat (Figure 4.4) displayed greater ($P < 0.05$) *PDK4* mRNA abundance in HWS than LWS chickens at 56 days, whereas there were no differences observed between the lines at day 28 in any of these tissues. There was a main effect of line on *PDK4* expression in clavicular fat ($P = 0.02$) where mRNA abundance was greater in LWS than HWS, irrespective of age. This was the only tissue for which expression was greater in LWS compared to HWS. There was an interaction of sex by line ($P = 0.002$) on *PDK4* abundance in hypothalamus, where HWS females expressed greater quantities of mRNA than HWS females and LWS males and females (Figure 4.5).

4.4.2 *FoxO1* expression in different tissues

FoxO1 showed differences in gene expression that were similar to *PDK4* (Table 4.2-Table 4.8) and similarly, there were no significant differences in the liver. The HWS

chickens had greater ($P < 0.01$) levels of *FoxO1* mRNA in both *Pectoralis major* and gastrocnemius, irrespective of age. In subcutaneous fat, there was greater ($P = 0.02$) expression of *FoxO1* mRNA in HWS at day 56 compared with LWS, and no difference between the lines at day 28 (Figure 4.6). In clavicular fat, there was an age x sex x line interaction on gene expression, where mRNA abundance was greater in LWS males at day 28 than for the other line-sex combinations (Figure 4.7). In the hypothalamus, there was a similar pattern causing the interaction, as mRNA was greatest at day 56 in LWS males than the others ($P < 0.05$, Figure 4.8).

4.4.3 *PPARγ* and *PGC1α* mRNA abundance in different tissues

PPARγ expression was similar for the genetic lines in abdominal fat and hypothalamus (Table 4.2-Table 4.8). Expression in liver was greater in HWS than in LWS ($P = 0.002$). For both *Pectoralis major* (Figure 4.9) and gastrocnemius (Figure 4.10), there was an interaction of age x line where expression was greater ($P < 0.05$) in LWS than HWS at day 28, with no differences between the lines at day 56. In *Pectoralis major* there was a line x sex interaction on *PPARγ* expression, where mRNA abundance was greater ($P < 0.05$) in LWS females than HWS females (Figure 4.11). There was a main effect of line on *PPARγ* mRNA in both clavicular fat and subcutaneous fat, with greater ($P < 0.05$) expression in LWS as compared to HWS chickens.

For *PGC1α*, the only significant difference between lines was in gastrocnemius, with an interaction of line x sex on mRNA ($P = 0.02$; Table 4.2-Table 4.8). In gastrocnemius, HWS males expressed higher levels of *PGC1α* than LWS males and HWS females (Figure 4.12).

4.5 Discussion

Down-regulation of *PDK4* and *FoxO1* and increased expression *PPARγ* could inhibit PDC phosphorylation in both white and red muscle fiber sub-types (Ashmore and Doerr, 1971; Strumilo, 2005). No major differences in gene expression were noted in 28-day-old chickens, although metabolic assays were not performed at this age. Changes between 28 and 56 days of age could be due to alterations in growth and body composition that occur during those four weeks. Also chronological age and physiological age may not be the same.

There are several mechanisms that may explain the regulatory function of *FoxO1* and *PPARγ* on *PDK4* in our model. In adipose tissue, *FoxO1* phosphorylation is reported to promote adipocyte differentiation (Accili and Arden, 2004; Gross et al., 2008). That may be the reason that we did not observe significant effects on *FoxO1* expression in highly differentiated abdominal fat. In the liver, both *FoxO1* and *PDK4* are linked to enhanced rates of gluconeogenesis in rodents (Postic et al., 2004). However, in the present study there was no change in either *PDK4* mRNA or *FoxO1* mRNA in the liver. This may be explained by the slightly different regulatory mechanisms in avian species or post transcription regulation. Further studies should attempt to measure hepatic gluconeogenic rates in HWS and LWS chickens at different ages, as well as differences in adipose tissue cellularity.

As endogenous *PPAR* ligands, free fatty acids and their derivatives have been implicated to be responsible for enhanced *PDK* expression in fasting and diabetes (Jeong et al., 2012). This was consistent with the greater fatty acid oxidation efficiency and relatively higher *PPARγ* mRNA expression in LWS fat tissues and skeletal muscle. As

for *PGC1α*, it was indicated that estrogen related receptor α (*ERRα*) is involved in *PDK4* promoter activation dependent on *PGC1α* in mouse C_2C_{12} cells (Wende et al., 2005; Araki and Motojima, 2006). *PDK4* can also be regulated by other molecular factors aside from these core factors.

In abdominal fat there was higher fatty acid oxidation efficiency in LWS, and this was also associated with greater activity of citrate synthase, a marker for mitochondrial content, and less expression of *PDK4*, consistent with greater flux through the β-oxidation pathway. Total palmitate oxidation was greater in HWS abdominal fat, consistent with the HWS being obese and having an overall greater capacity for energy oxidation. While metabolic activities were not measured in clavicular fat (another organ-associated fat depot) or subcutaneous fat, both depots showed different patterns of gene expression, where *PDK4* mRNA was greater in LWS and HWS, respectively, while for *PPARγ*, expression was greater in LWS in both fat depots. Yet for all tissues where *FoxO1* expression was greater in HWS (subcutaneous fat and both skeletal muscle tissues), there was also greater expression of *PDK4* in HWS, suggestive of coordinate regulation. While metabolic and histological assays were performed only on males, the gene expression differences for *PPARγ* and *PGC1α* in males and females suggest that there could be effects of body composition in juveniles on metabolism that are influenced by gender.

The striking differences in oxidative metabolism in abdominal fat, coupled to differences in gene expression that were fat-depot specific, raise the question of whether fat deposition occurs by hyperplasia or hypertrophy. Further studies are needed to elucidate the cellular mechanisms underlying fat development in HWS and LWS.

Table 4.1 Real Time PCR primer sequences.

Gene[1]	Accession No.	Sequences (5' → 3')[2]
β *actin*	NM_205518.1	F: GTCCACCGCAAATGCTTCTAA R: TGCGCATTTATGGGTTTTGTT
PDK4	NM_001199909.1	F: GCTGGACTTCGGCTCGACTA R: TCGCAGGAACGCAAAGG
FoxO1	NM_204328.1	F: GCCTCCTTTTTCGAGGGTGTT R: GCGGTATGTACATGCCAATCTC
PPARγ	NM_001001460.1	F: CACTGCAGGAACAGAACAAAGAA R: TCCACAGAGCGAAACTGACATC
PGC1α	NM_001006457.1	F: GAGGATGGATTGCCTTCATTTG R: GCGTCATGTTCATTGGTCACA

[1]*PDK4* = pyruvate dehydrogenase kinase 4, *FoxO1* = forkhead box O1A, *PPARγ* = peroxisome proliferator-activated receptor γ, *PGC1α* = peroxisome proliferator-activated receptor γ coactivator α.

[2]F = forward, R = reverse.

Table 4.2 mRNA abundance in hypothalamus of 28- and 56-day-old HWS and LWS chickens.

Hypothalamus		Relative Gene Expression[2]			
		PDK4	*FoxO1*	*PPARγ*	*PGC1α*
Line (n=10)	LWS	1.0965	0.6642	0.5535	0.7328
	HWS	1.6278	0.5130	0.6946	0.9302
	SEM	0.0917	0.0507	0.0884	0.0709
	P-value	**0.0002**	**0.0420**	0.2667	0.0567
Age (n=10)	Day28	1.2216	0.6320	0.7220	0.8221
	Day56	1.4889	0.5488	0.5075	0.8310
	SEM	0.1065	0.0528	0.0863	0.0746
	P-value	0.0845	0.2728	0.0875	0.9335
Sex (n=10)	Female	1.3589	0.5974	0.5749	0.7392
	Male	1.3386	0.5882	0.6613	0.9047
	SEM	0.1110	0.0537	0.0894	0.0720
	P-value	0.8981	0.9042	0.4984	0.1128
Interaction[1]	L ×A	**0.0002**	0.0690	0.2358	0.2226
	L ×S	**0.0002**	0.0862	0.6196	0.1141
	A ×S	0.3561	0.3533	0.3237	0.4830
	L ×A ×S	**<0.0001**	**0.0241**	0.6437	0.4565

Data are shown as least squares means ± standard errors of the means.

[1] For the interaction, L, A and S represent the effects of line, age and sex, respectively.

[2] *PDK4* = pyruvate dehydrogenase kinase 4, *FoxO1* = forkhead box O1A, *PPARγ* = peroxisome proliferator-activated receptorγ, *PGC1α* = peroxisome proliferator-activated receptor γ coactivator α.

Table 4.3 mRNA abundance in liver of 28- and 56-day-old HWS and LWS chickens.

Liver		Relative Gene Expression[2]			
		PDK4	*FoxO1*	*PPARγ*	*PGC1α*
Line (n=10)	LWS	0.0774	0.2279	0.0401	0.2702
	HWS	0.0660	0.1968	0.0748	0.1486
	SEM	0.0119	0.0307	0.0073	0.0446
	P-value	0.5010	0.4778	**0.0017**	0.0616
Age (n=10)	Day28	0.0492	0.1655	0.0597	0.1442
	Day56	0.0941	0.2592	0.0552	0.2746
	SEM	0.0108	0.0289	0.0083	0.0443
	P-value	**0.0055**	**0.0276**	0.7048	**0.0440**
Sex (n=10)	Female	0.0749	0.1596	0.0546	0.2041
	Male	0.0684	0.2651	0.0603	0.2147
	SEM	0.0119	0.0284	0.0083	0.0467
	P-value	0.7021	**0.0124**	0.6256	0.8725
Interaction[1]	L ×A	**0.0262**	0.1138	**0.0113**	**0.0090**
	L ×S	0.7338	0.0621	**0.0188**	0.2569
	A ×S	**0.0498**	**0.0006**	0.8202	0.2477
	L ×A ×S	0.1951	**0.0035**	**0.0415**	0.1054

Data are shown as least squares means ± standard errors of the means.

[1] For the interaction, L, A and S represent the effects of line, age and sex, respectively.

[2] *PDK4* = pyruvate dehydrogenase kinase 4, *FoxO1* = forkhead box O1A, *PPARγ* = peroxisome proliferator-activated receptorγ, *PGC1α* = peroxisome proliferator-activated receptor γ coactivator α.

Table 4.4 mRNA abundance in *Pectoralis major* of 28- and 56-day-old HWS and LWS chickens.

Pectoralis major		Relative Gene Expression[2]			
		PDK4	*FoxO1*	*PPARγ*	*PGC1α*
Line (n=10)	LWS	0.0130	0.0687	0.0892	0.6488
	HWS	0.0363	0.1275	0.0696	0.5796
	SEM	0.0055	0.0137	0.0054	0.0787
	P-value	**0.0047**	**0.0043**	**0.0142**	0.5382
Age (n=10)	Day28	0.0138	0.0728	0.0809	0.5247
	Day56	0.0344	0.1207	0.0784	0.7009
	SEM	0.0056	0.0142	0.0059	0.0764
	P-value	**0.0131**	**0.0226**	0.7651	**0.1114**
Sex (n=10)	Female	0.0272	0.0856	0.0831	0.5121
	Male	0.0216	0.1084	0.0764	0.7130
	SEM	0.0061	0.0151	0.0058	0.0755
	P-value	0.5183	0.2913	0.4242	0.0679
Interaction[1]	L ×A	**0.0001**	**0.0024**	**0.0199**	0.0813
	L ×S	**0.0379**	**0.0217**	**0.0139**	0.2942
	A ×S	0.0932	**0.0072**	0.8651	0.1052
	L ×A ×S	**0.0014**	**0.0014**	**0.0426**	0.0711

Data are shown as least squares means ± standard errors of the means.

[1] For the interaction, L, A and S represent the effects of line, age and sex, respectively.

[2] *PDK4* = pyruvate dehydrogenase kinase 4, *FoxO1* = forkhead box O1A, *PPARγ* = peroxisome proliferator-activated receptorγ, *PGC1α* = peroxisome proliferator-activated receptor γ coactivator α.

Table 4.5 mRNA abundance in gastrocnemius of 28- and 56-day-old HWS and LWS chickens.

Gastrocnemius		Relative Gene Expression[2]			
		PDK4	*FoxO1*	*PPARγ*	*PGC1α*
Line (n=10)	LWS	0.0046	0.1365	0.0689	0.3752
	HWS	0.0227	0.2908	0.0363	0.6003
	SEM	0.0041	0.0301	0.0080	0.0997
	P-value	**0.0033**	**0.0009**	**0.0067**	0.1190
Age (n=10)	Day28	0.0039	0.1953	0.0646	0.3117
	Day56	0.0234	0.2349	0.0404	0.6607
	SEM	0.0040	0.0348	0.0084	0.0948
	P-value	**0.0015**	0.4258	**0.0491**	**0.0132**
Sex (n=10)	Female	0.0113	0.1773	0.0516	0.3830
	Male	0.0164	0.2520	0.0528	0.5929
	SEM	0.0046	0.0340	0.0089	0.1002
	P-value	0.4340	0.1281	0.9239	0.1471
Interaction[1]	L ×A	**<0.0001**	**0.0055**	**0.0009**	**0.0146**
	L ×S	**0.0146**	**0.0021**	0.0572	**0.0263**
	A ×S	**0.0083**	0.0807	0.2854	**0.0301**
	L ×A ×S	**<0.0001**	**0.0026**	**0.0220**	**0.0043**

Data are shown as least squares means ± standard errors of the means.

[1] For the interaction, L, A and S represent the effects of line, age and sex, respectively.

[2] *PDK4* = pyruvate dehydrogenase kinase 4, *FoxO1* = forkhead box O1A, *PPARγ* = peroxisome proliferator-activated receptorγ, *PGC1α* = peroxisome proliferator-activated receptor γ coactivator α.

Table 4.6 mRNA abundance in abdominal fat of 28- and 56-day-old HWS and LWS chickens.

Abdominal fat		Relative Gene Expression[2]			
		PDK4	*FoxO1*	*PPARγ*	*PGC1α*
Line (n=10)	LWS	0.0607	0.5438	0.0062	38.6487
	HWS	0.0983	0.7413	0.0047	40.3142
	SEM	0.0180	0.1121	0.0026	9.7246
	P-value	0.1495	0.2235	0.6857	0.9047
Age (n=10)	Day28	0.0624	0.8132	0.0086	49.8435
	Day56	0.0971	0.5429	0.0029	32.0654
	SEM	0.0181	0.1097	0.0025	9.4627
	P-value	0.1855	0.0922	0.1096	0.1950
Sex (n=10)	Female	0.1026	0.6233	0.0064	27.4707
	Male	0.0633	0.6898	0.0043	51.0306
	SEM	0.0177	0.1136	0.0025	9.1700
	P-value	0.1268	0.6821	0.5670	0.0790
Interaction[1]	L ×A	**0.0063**	0.1488	0.2029	0.5334
	L ×S	0.1418	0.3242	0.5103	0.3631
	A ×S	0.2402	0.3469	0.3998	0.1003
	L ×A ×S	**0.0197**	0.4085	0.3167	0.5121

Data are shown as least squares means ± standard errors of the means.

[1] For the interaction, L, A and S represent the effects of line, age and sex, respectively.

[2] *PDK4* = pyruvate dehydrogenase kinase 4, *FoxO1* = forkhead box O1A, *PPARγ* = peroxisome proliferator-activated receptorγ, *PGC1α* = peroxisome proliferator-activated receptor γ coactivator α.

Table 4.7 mRNA abundance in clavicular fat of 28- and 56-day-old HWS and LWS chickens.

Clavicular fat		Relative Gene Expression[2]			
		PDK4	*FoxO1*	*PPARγ*	*PGC1α*
Line (n=10)	LWS	0.3710	1.2288	0.0170	24.4096
	HWS	0.1024	0.7200	0.0039	34.3881
	SEM	0.0787	0.1608	0.0039	5.6640
	P-value	**0.0217**	**0.0324**	**0.0218**	0.2221
Age (n=10)	Day28	0.2097	1.1303	0.0102	35.5200
	Day56	0.2458	0.8076	0.0099	24.5121
	SEM	0.0854	0.1681	0.0042	5.6341
	P-value	0.7671	0.1842	0.9497	0.1769
Sex (n=10)	Female	0.2406	0.7485	0.0121	25.2568
	Male	0.2169	1.1704	0.0080	34.1279
	SEM	0.0854	0.1644	0.0042	5.6849
	P-value	0.8456	0.0790	0.4876	0.2781
Interaction[1]	L ×A	0.1282	**0.0008**	0.1498	0.3694
	L ×S	0.1428	**0.0121**	0.0614	0.1129
	A ×S	0.3998	**0.0050**	0.7067	0.2669
	L ×A ×S	0.1505	**<0.0001**	0.2874	0.1502

Data are shown as least squares means ± standard errors of the means.

[1] For the interaction, L, A and S represent the effects of line, age and sex, respectively.

[2] *PDK4* = pyruvate dehydrogenase kinase 4, *FoxO1* = forkhead box O1A, *PPARγ* = peroxisome proliferator-activated receptorγ, *PGC1α* = peroxisome proliferator-activated receptor γ coactivator α.

Table 4.8 mRNA abundance in subcutaneous fat of 28- and 56-day-old HWS and LWS chickens.

Subcutaneous fat		Relative Gene Expression[2]			
		PDK4	*FoxO1*	*PPARγ*	*PGC1α*
Line (n=10)	LWS	0.0560	0.4476	0.0082	14.4280
	HWS	0.1711	0.6289	0.0041	25.5337
	SEM	0.0434	0.0507	0.0007	4.2805
	P-value	0.0881	**0.0280**	**0.0004**	0.0947
Age (n=10)	Day28	0.0586	0.5149	0.0047	25.2335
	Day56	0.2356	0.6675	0.0052	21.2064
	SEM	0.0293	0.0438	0.0008	3.8498
	P-value	**0.0003**	**0.0222**	0.6405	0.4673
Sex (n=10)	Female	0.1517	0.5876	0.0061	20.7895
	Male	0.1417	0.5954	0.0036	26.0923
	SEM	0.0397	0.0496	0.0007	3.8251
	P-value	0.8597	0.9132	**0.0173**	0.3380
Interaction[1]	L ×A	**<0.0001**	**0.0013**	**0.0043**	0.2890
	L ×S	**0.0054**	0.0630	0.1388	0.7205
	A ×S	0.3523	0.1156	**0.0002**	0.2386
	L ×A ×S	**0.0022**	**0.0083**	**0.0020**	0.6086

Data are shown as least squares means ± standard errors of the means.

[1] For the interaction, L, A and S represent the effects of line, age and sex, respectively.

[2] *PDK4* = pyruvate dehydrogenase kinase 4, *FoxO1* = forkhead box O1A, *PPARγ* = peroxisome proliferator-activated receptorγ, *PGC1α* = peroxisome proliferator-activated receptor γ coactivator α.

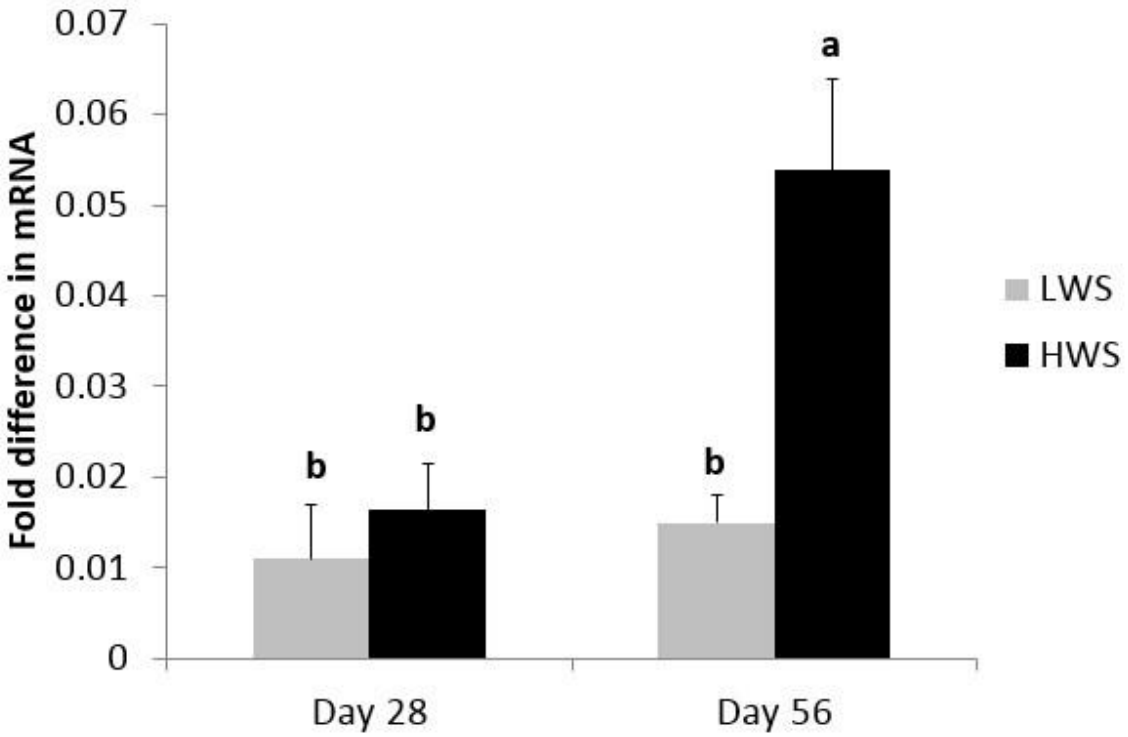

Figure 4.1 Relative *PDK4* mRNA abundance in *Pectoralis major* of 28- and 56-day-old HWS and LWS chickens. n=10. There was a two-way interaction of age x genetic line. $P = 0.0165$. Bars with different letters represent a significant difference, $P < 0.05$. Values represent least squares means ± SEM.

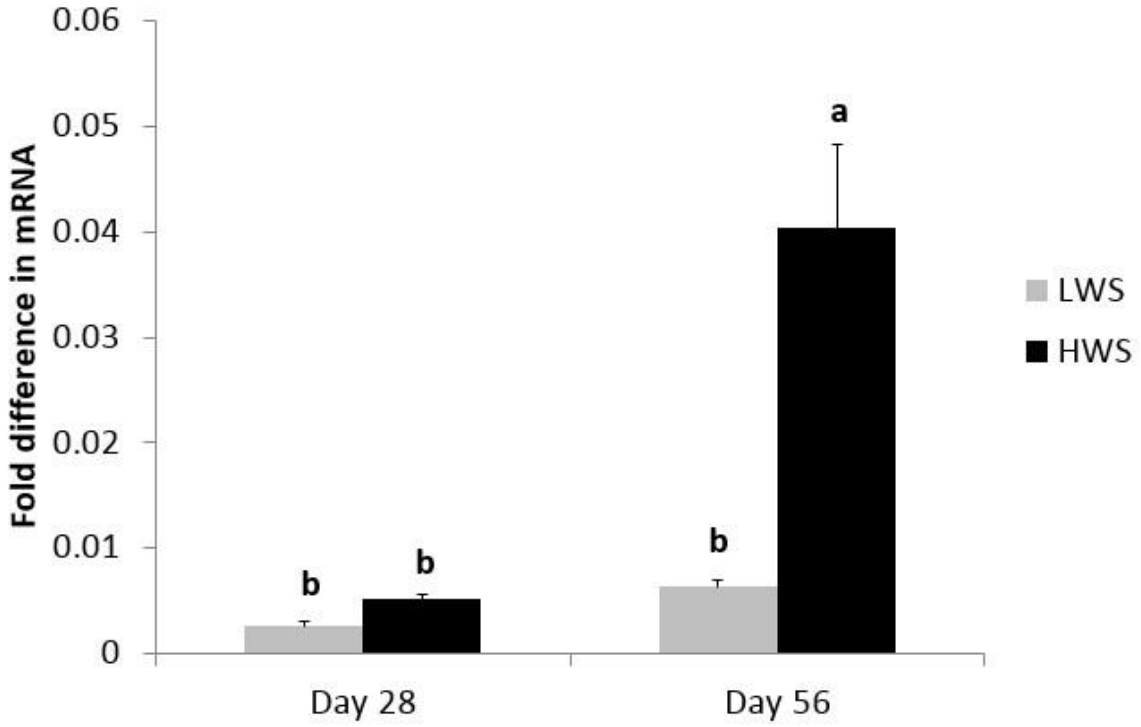

Figure 4.2 Relative *PDK4* mRNA abundance in gastrocnemius of 28- and 56-day-old HWS and LWS chickens. n=10. There was a two-way interaction of age x genetic line. P=0.0030. Bars with different letters represent a significant difference, $P < 0.05$. Values represent least squares means ± SEM.

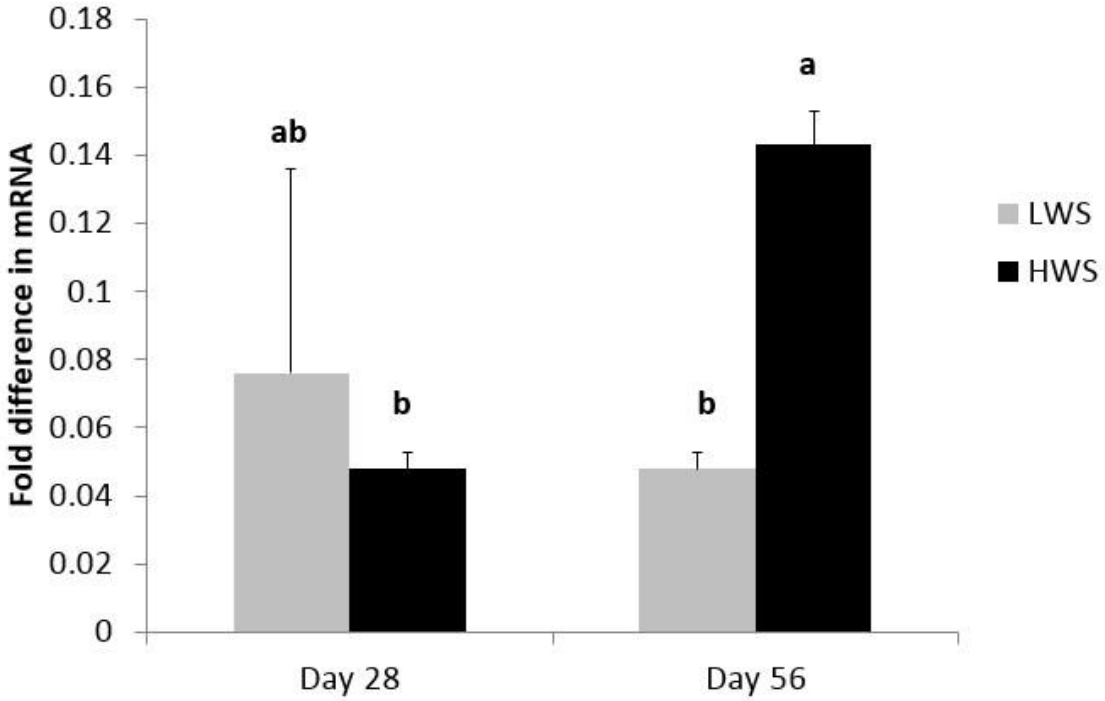

Figure 4.3 Relative *PDK4* mRNA abundance in abdominal fat of 28- and 56-day-old HWS and LWS chickens. n=10. There was a two-way interaction of age x genetic line. P=0.0108. Bars with different letters represent a significant difference, $P < 0.05$. Values represent least squares means ± SEM.

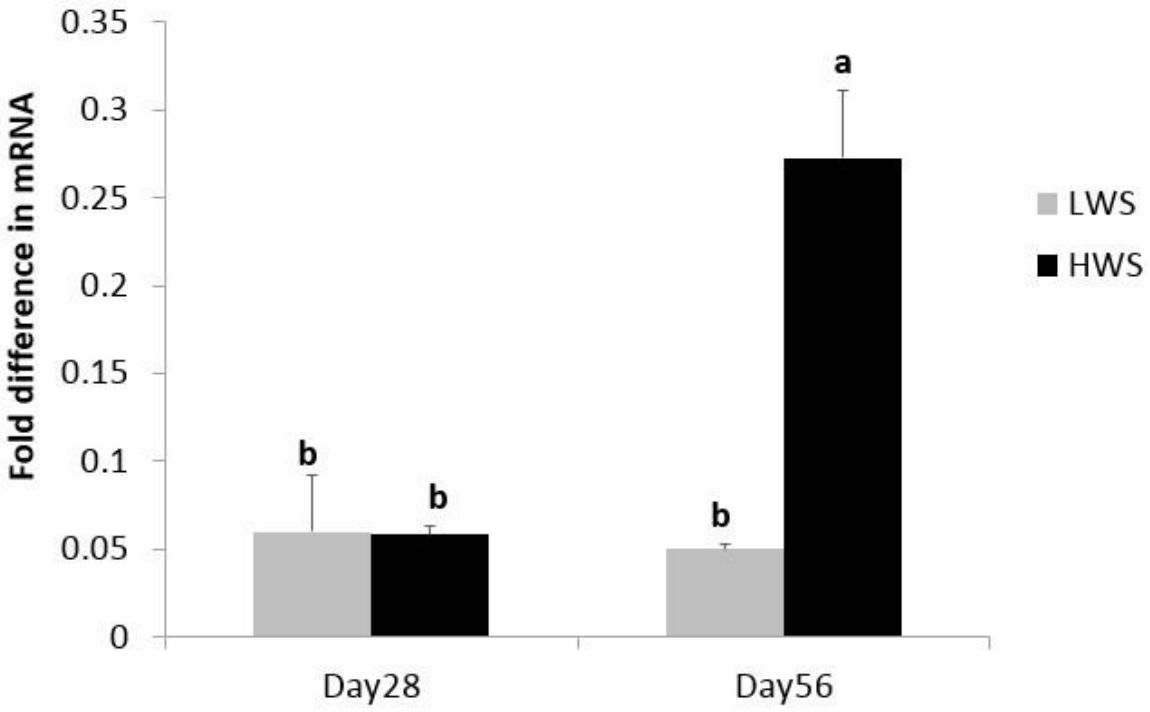

Figure 4.4 Relative *PDK4* mRNA abundance in subcutaneous fat of 28- and 56-day-old HWS and LWS chickens. n=10. There was a two-way interaction of age x genetic line. P=0.0176. Bars with different letters represent a significant difference, $P < 0.05$. Values represent least squares means ± SEM.

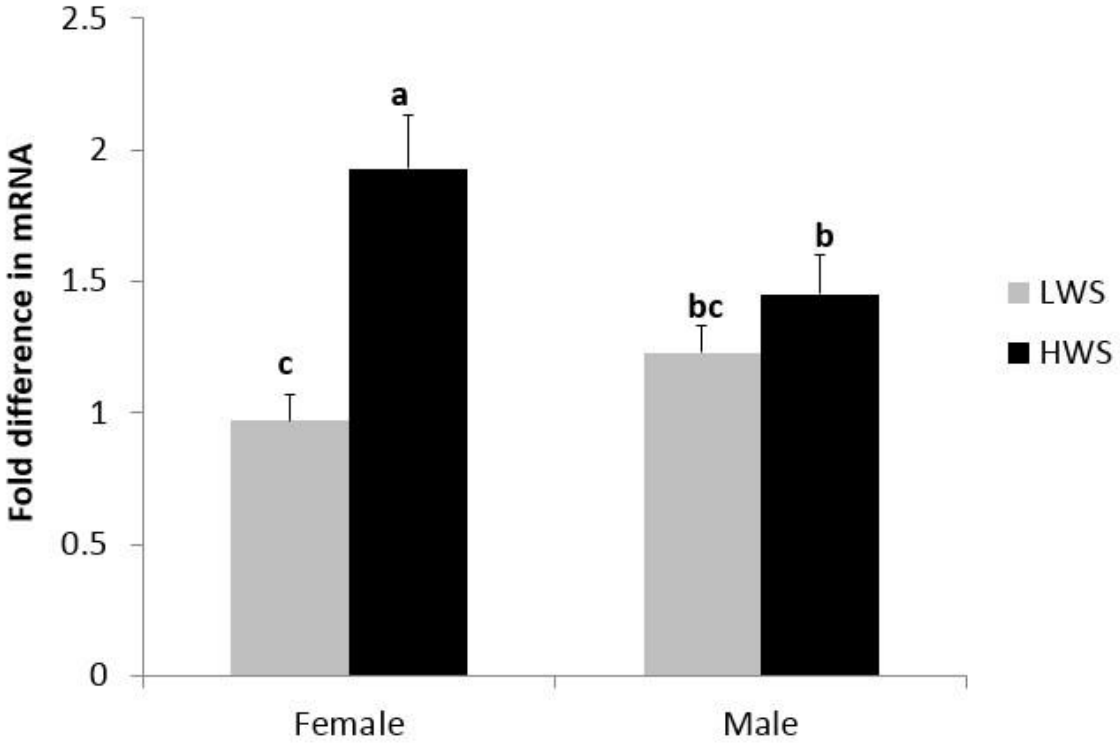

Figure 4.5 Relative *PDK4* mRNA abundance in hypothalamus of 28- and 56-day-old HWS and LWS chickens. n=10. There was a two-way interaction of sex x genetic line. P=0.0019. Bars with different letters represent a significant difference, $P < 0.05$. Values represent least squares means ± SEM.

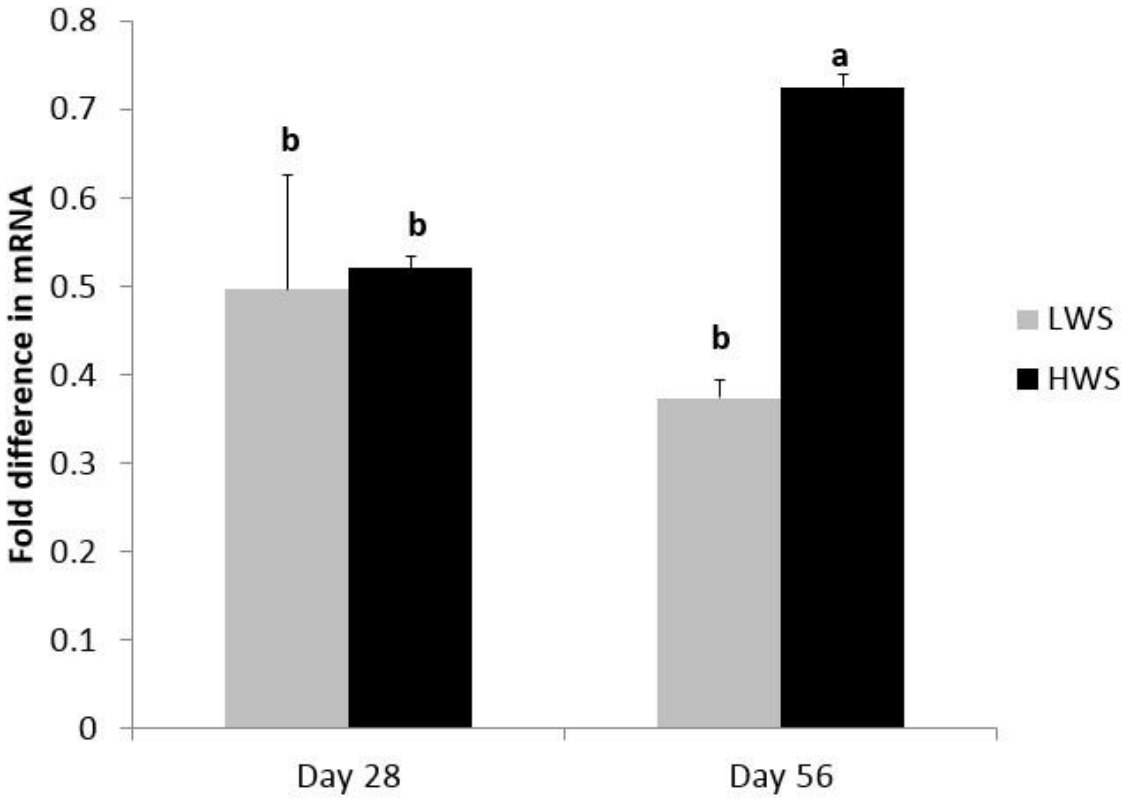

Figure 4.6 Relative *FoxO1* mRNA abundance in subcutaneous fat of 28- and 56-day-old HWS and LWS chickens. n=10. There was a two-way interaction of age x genetic line. P=0.0166. Bars with different letters represent a significant difference, $P < 0.05$. Values represent least squares means ± SEM.

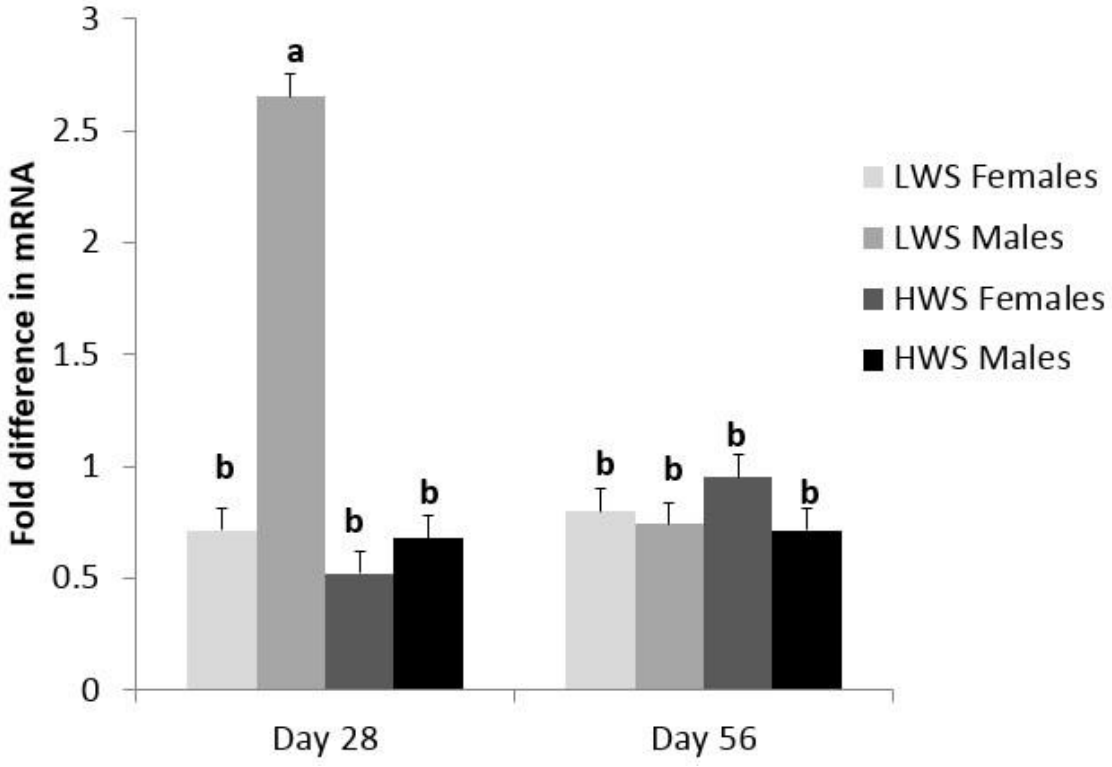

Figure 4.7 Relative *FoxO1* mRNA abundance in clavicular fat of 28- and 56-day-old HWS and LWS chickens. n=10. There was a three-way interaction of age x sex x genetic line. P=0.0015. Bars with different letters represent a significant difference, $P < 0.05$. Values represent least squares means ± SEM.

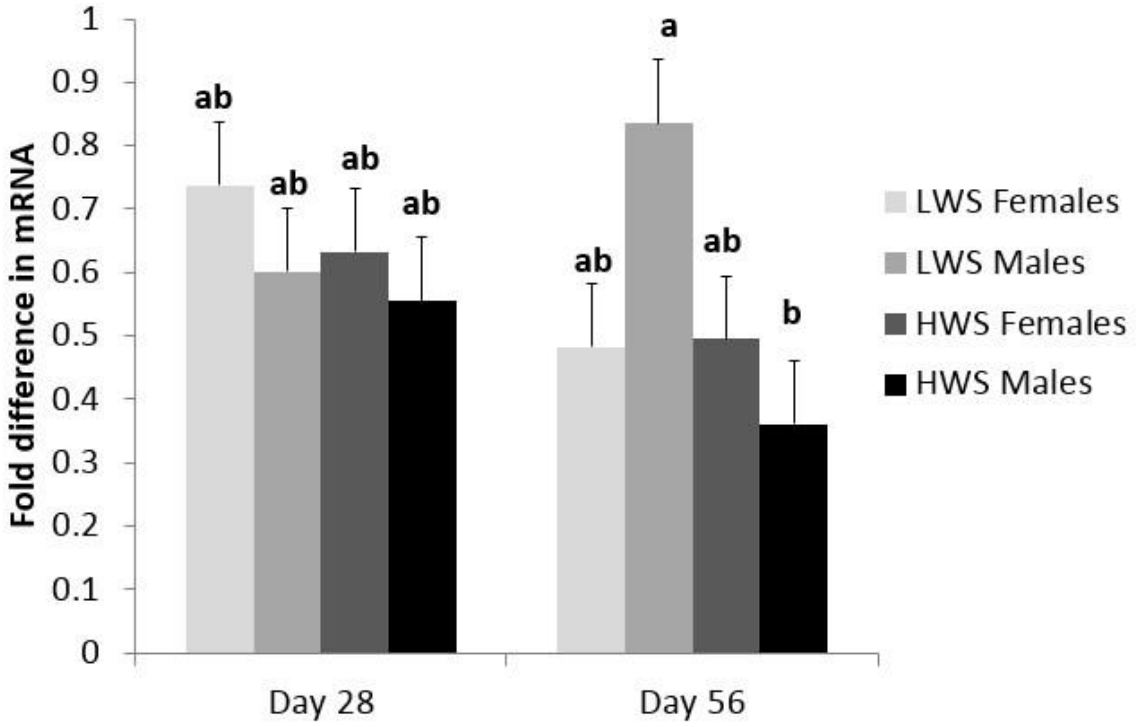

Figure 4.8 Relative *FoxO1* mRNA abundance in hypothalamus of 28- and 56-day-old HWS and LWS chickens. n=10. There was a three-way interaction of age x sex x genetic line. P=0.0467. Bars with different letters represent a significant difference, $P < 0.05$. Values represent least squares means ± SEM.

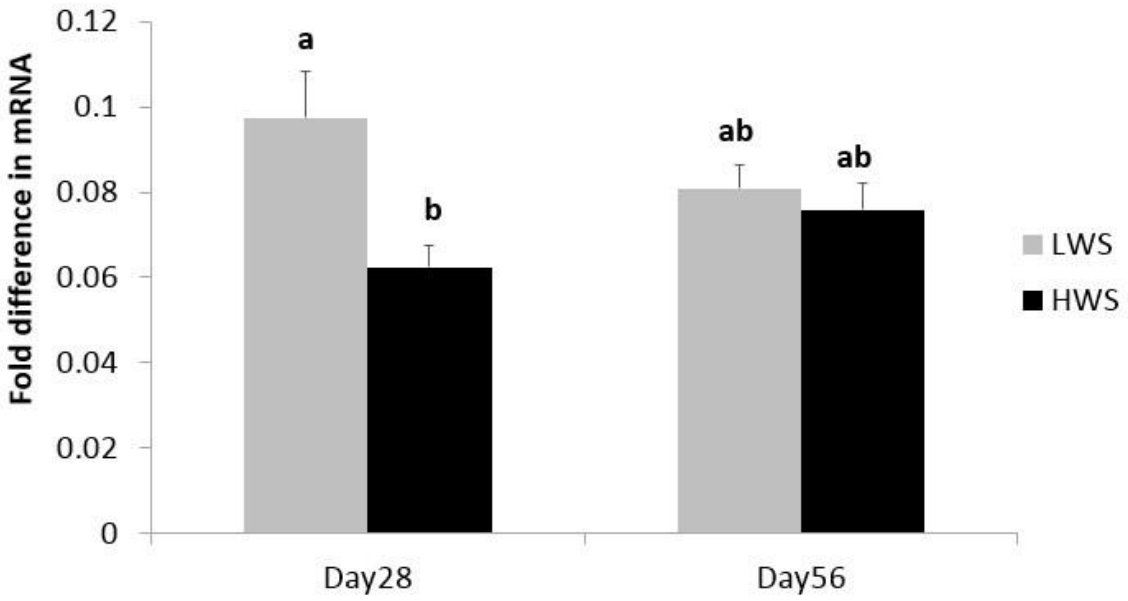

Figure 4.9 Relative *PPARγ* mRNA abundance in *Pectoralis major* of 28- and 56-day-old HWS and LWS chickens. n=10. There was a two-way interaction of age x genetic line. *P*=0.0442. Bars with different letters represent a significant difference, $P < 0.05$. Values represent least squares means ± SEM.

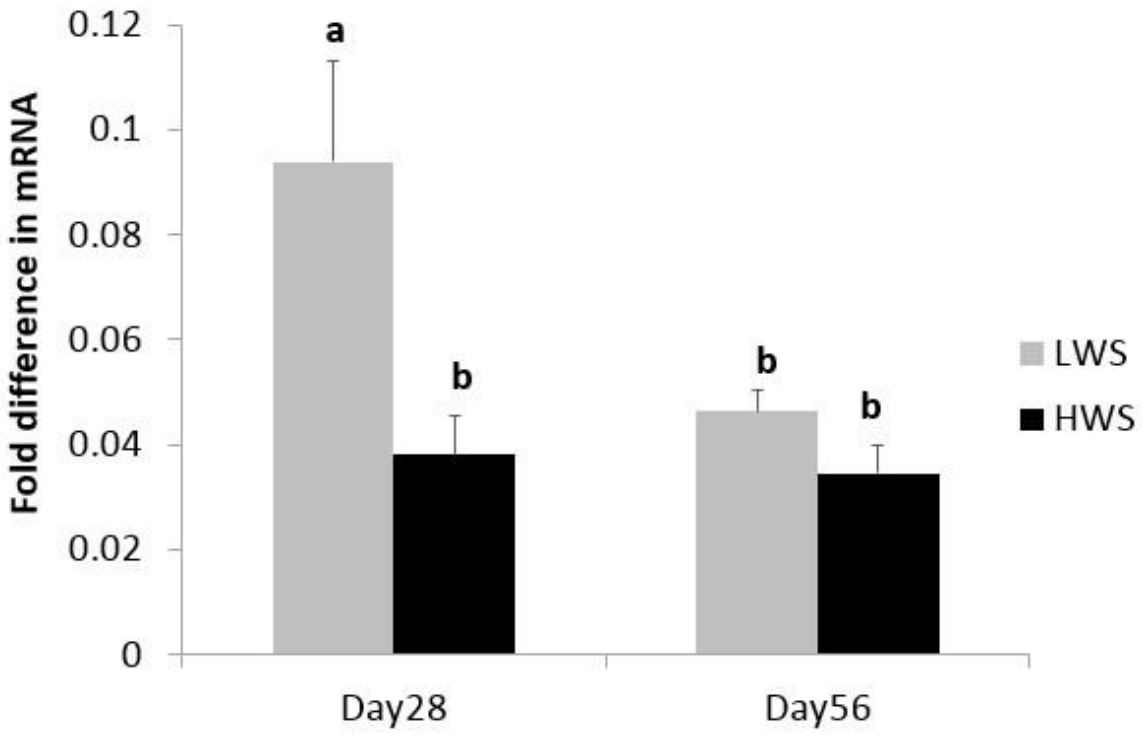

Figure 4.10 Relative *PPARγ* mRNA abundance in gastrocnemius of 28- and 56-day-old HWS and LWS chickens. n=10. There was a two-way interaction of age x genetic line. *P*=0.0457. Bars with different letters represent a significant difference, $P < 0.05$. Values represent least squares means ± SEM.

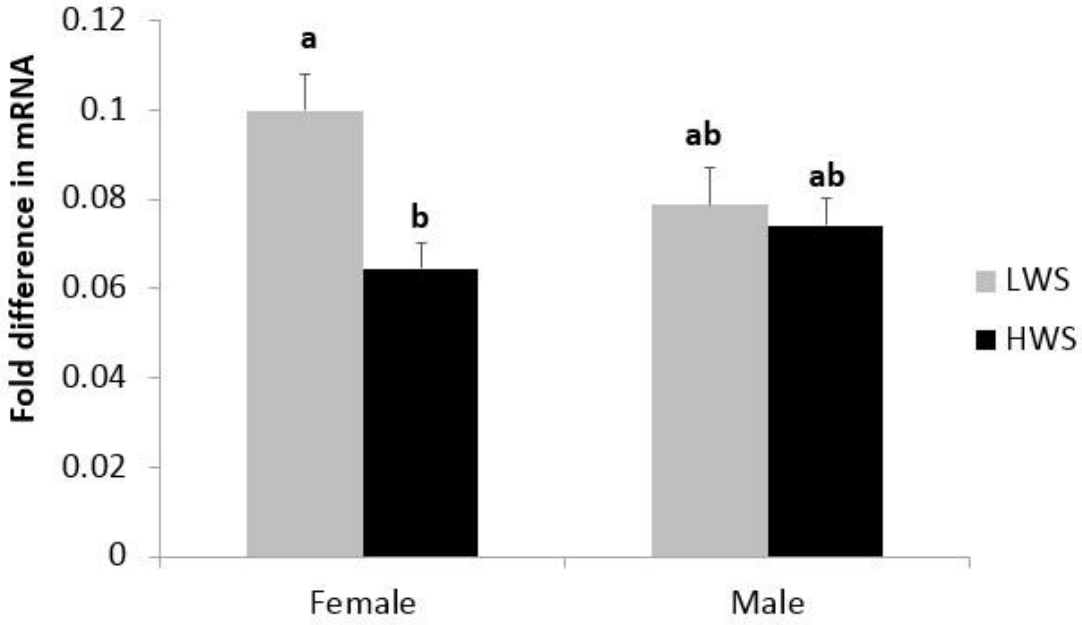

Figure 4.11 Relative *PPARγ* mRNA abundance in *Pectoralis major* of 28- and 56-day-old HWS and LWS chickens. n=10. There was a two-way interaction of sex x genetic line. *P*=0.0397. Bars with different letters represent a significant difference, $P < 0.05$. Values represent least squares means ± SEM.

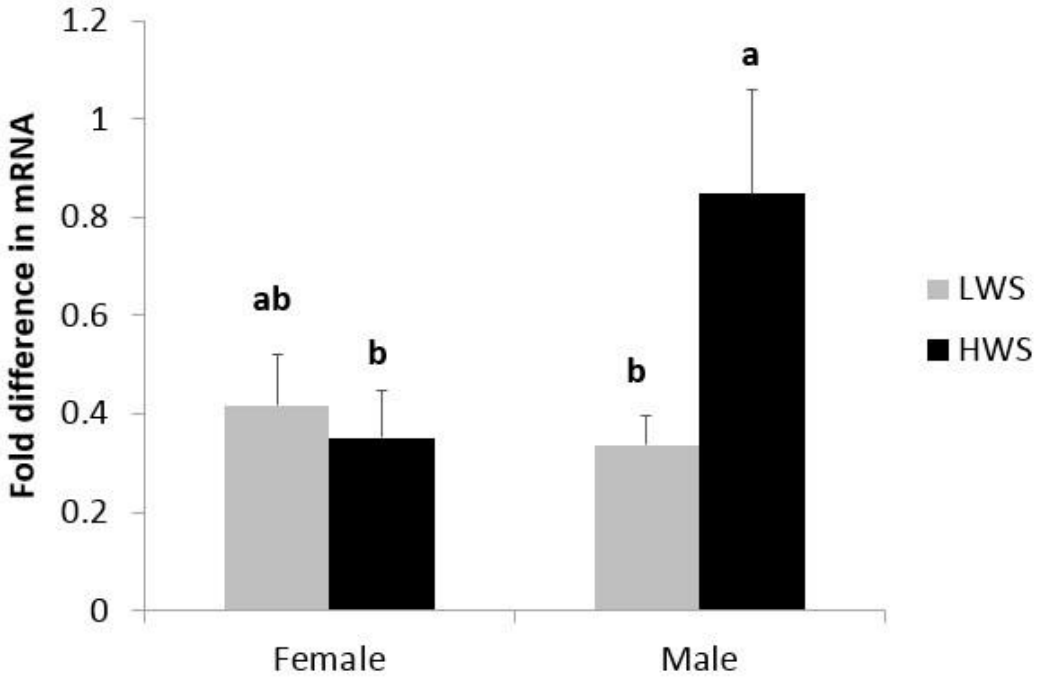

Figure 4.12 Relative *PGC1α* mRNA abundance in gastrocnemius of 28- and 56-day-old HWS and LWS chickens. n=10. There was a two-way interaction of sex x genetic line. P=0.0228. Bars with different letters represent a significant difference, $P < 0.05$. Values represent least squares means ± SEM.

CHAPTER 5 Chickens Selected for High or Low Body Weight Differ in Adipocyte Cellularity in Different Adipose Tissues

5.1 Abstract

The Virginia lines of chickens are a unique model of hypophagia and obesity that have resulted from long-term (56 generations) divergent selection for high (HWS) or low (LWS) juvenile (56 days of age) body weight, respectively. Selection for body weight, with a more than tenfold difference in body weight now observed between the lines at selection age, led to correlated responses in body composition. We hypothesized that there are significant differences in adipocyte cellularity in different white adipose tissues between HWS and LWS chickens. At day 65, randomly selected male HWS and LWS chickens (n = 9) were euthanized and abdominal fat, clavicular fat and subcutaneous fat were collected for histological analysis. Images were captured and analyzed with NIS-Elements Advanced Research Software (Nikon). The threshold method was used to count adipocytes. Adipocytes were treated as binary objects with the restriction that measurements must exceed 100 μm^2. The mean area, mean equivalent diameter (EqDiameter) and mean circularity of each object and the total object numbers as well as the total area were recorded. Object density and the size distribution pattern in each image were also analyzed. The statistical model included the effects of fat depot (abdominal or clavicular fat), genetic line (HWS and LWS), and the interaction between them. Data were analyzed by ANOVA using JMP 10.0 and the Fit Model platform. Means were separated using Tukey's Test. Adipocyte areas were greater in HWS than in LWS for abdominal ($P < 0.0001$) and clavicular fat ($P < 0.0001$). In HWS, adipocytes were largest in clavicular fat, smallest in subcutaneous fat and intermediate in abdominal

fat ($P < 0.01$). The mean diameters of fat cells showed similar differences, being greater in HWS abdominal ($P < 0.0001$) and clavicular fat ($P < 0.0001$) compared to LWS. The patterns were similar for adipocyte diameter between fat depots in HWS, with largest cells in clavicular fat and smallest in subcutaneous fat. Overall cellular density was greater ($P < 0.0001$) in LWS than in HWS in both abdominal fat and clavicular fat. In HWS there were more adipocytes per unit area in subcutaneous fat than clavicular fat ($P < 0.01$). There was not enough subcutaneous fat to sample from LWS, thus subcutaneous fat data are reported only for the HWS chickens. Most of the adipocytes in HWS fat samples were between 1,000 and 4,000 μm^2, with adipocytes as large as 9,500 μm^2. The LWS, on the other hand, contained greater numbers of small cells, with most adipocytes between 500 and 2,000 μm^2, and no adipocytes larger than 5,200 μm^2. The results show that the adipocytes in all three adipose tissues of HWS chickens were larger and sparser as compared to the LWS adipocytes. There were also "oversized" adipocytes in abdominal fat and clavicular fat in HWS chickens, which are possible markers for inflammation and insulin resistance.

5.2 Introduction

Different nutritional states can affect lipid accumulation in poultry and mammals. Broilers fed *ad libitum* increase the weight of abdominal fat predominantly through hyperplasia while selectively refilling existing adipocytes after starvation and re-feeding (March and Hansen, 1977). In mammalian models of obesity, there are differences described for visceral and subcutaneous fat, with visceral fat being described as more metabolically-active and associated with inflammation and the subcutaneous fat being relatively benign. Abdominal fat has higher activities of both lipogenesis and lipolysis, and its accumulation can induce high levels of free fatty acids (FFA). The extra FFA may cause the enhancement of lipid synthesis and gluconeogenesis as well as insulin resistance, resulting in hyperlipidemia, glucose intolerance and hypertension and finally atherosclerosis (Matsuzawa et al., 1995). However, subcutaneous fat showed an independent negative correlation with glucose and atherogenic lipid components, with less gene expression related to glucose homeostasis, insulin action and lipid metabolism (Hamdy et al., 2006). Moreover, it is hypothesized that much of the expansion of adipose tissue in obesity is due to a mixed contribution of hyperplasia and hypertrophy in the visceral-associated depots. It is described as a kind of pathological expansion of adipocytes with enlargement of existing fat cells, a high degree of macrophage infiltration, limited vessel development, massive fibrosis and chronic inflammation (Sun et al., 2011).

In the present study, we evaluated adipocyte morphology in the 65-day-old Virginia lines of chickens that have resulted from long-term (56 generations) divergent selection for high (HWS) or low (LWS) juvenile body weight. Selection for body weight,

with a more than tenfold difference in body weight now observed between the lines at selection age, led to correlated responses in body composition, and our previous studies showed that there are differences in fatty acid oxidation and gene expression in different adipose tissue depots of HWS and LWS. We hypothesized that there are significant differences in adipocyte cellularity in different white adipose tissues (abdominal fat, clavicular fat, and subcutaneous fat) between HWS and LWS chickens.

5.3 Materials and Methods

5.3.1 Animals

The details about the animals used in this study are the same as described in 3.3.1.

5.3.2 Adipose tissue histology

At day 65, 9 LWS and 9 HWS randomly selected male chickens were euthanized by cervical dislocation and abdominal fat, clavicular fat and subcutaneous fat removed, rinsed in PBS and submerged and fixed in neutral-buffered formalin, and tubes transferred to 4°C for overnight incubation. Samples were then dehydrated in a graded ethanol series, paraffin embedded, sectioned at 5 μm and mounted with hemotoxylin and eosin stained. For each chicken, fat was sectioned at three locations in the tissue, with three sections mounted per slide. Images were captured with a Nikon Eclipse 80i microscope and DS-Ri1 super high-definition cooled color camera head, and images analyzed using NIS-Elements Advanced Research Software (Nikon). For the analysis, three images were captured on each section of each slide, and the density and area of all adipocytes within the field of an image were measured under 20x magnification. The threshold method was used to count adipocytes. Adipocytes were treated as binary

objects with the restriction that measurements must exceed 100 μm^2. The mean area, mean equivalent diameter (EqDiameter) and mean circularity of each object and the total object numbers as well as the total area were recorded. Object density and the size distribution pattern in each image were also analyzed.

5.3.3 Statistical analysis

The statistical model for the adipocyte area and diameter data included the effects of fat depot, genetic line, and the interaction between them. Because the LWS did not have subcutaneous fat, the subcutaneous fat data were analyzed only for HWS in a separate analysis where the model included the effects of tissue depot. For all analyses, data normality and heterogeneity of variances were evaluated then ANOVA performed using JMP Pro version 10.0 (SAS Institute, USA) and the Fit Model platform. Means were separated using Tukey's Test. Data are presented as least square means ± SEM and statistical significance assigned at $P < 0.05$.

5.4 Results

Representative images of adipose tissue cross-sections are displayed in Figure 5.1 and the adipocyte cellularity data are shown in Table 5.1 and Table 5.2. Adipocyte areas were greater in HWS than in LWS for abdominal ($P < 0.0001$) and clavicular fat ($P < 0.0001$; Figure 5.2). In HWS, adipocytes were largest in clavicular fat, smallest in subcutaneous fat and intermediate in abdominal fat ($P < 0.01$). The mean diameters of fat cells showed similar differences, being greater in HWS abdominal ($P < 0.0001$) and clavicular fat ($P < 0.0001$; Figure 5.3). The patterns were similar for adipocyte diameter between fat depots in HWS, being greatest in clavicular fat and smallest in subcutaneous

fat (Figure 5.3). Overall cellular density was greater ($P < 0.0001$) in LWS than in HWS in both abdominal fat and clavicular fat (Figure 5.4). In HWS there were more adipocytes per unit area in subcutaneous fat than clavicular fat ($P < 0.01$). There was not enough subcutaneous fat to sample from LWS, thus subcutaneous fat data are reported only for the HWS chickens.

General size distribution of adipocytes among fat tissues within the same line followed a similar pattern (Figure 5.5). Most of the adipocytes in HWS fat samples were between 1,000 and 4,000 μm^2, with adipocytes as large as 9,500 μm^2 (Figure 5.5). The LWS, on the other hand, contained greater numbers of small cells, with most adipocytes between 500 and 2,000 μm^2, and no adipocytes larger than 5,200 μm^2.

5.5 Discussion

The adipocytes in all three adipose tissues of HWS chickens were larger and sparser as compared to the LWS adipocytes. There were also "oversized" adipocytes in abdominal fat and clavicular fat in HWS chickens, which are described as being markers for inflammation and insulin resistance (Maffeis et al., 2007). In the present study, the adipose tissue cross-sections were closely inspected for gross signs of immune cell infiltration and inflammation because an imbalance or dysfunction of adipose tissue can exacerbate obesity-related inflammation, which in turn results in energy metabolism disorders (Meijer et al., 2011). However, we didn't detect any signs of immune cell infiltration and inflammation in adipose tissues from HWS chickens. This histology analysis provided one explanation for the relative impairment in fatty acid oxidation efficiency and metabolic flexibility in HWS chickens. These results are consistent with those reported in an experiment conducted with 280 day-old chickens from the 29th

generation of selection (Robey et al., 1992). In that study, HWS and LWS males were fed ad-libitum or force-fed for 18 days and abdominal fat samples revealed that LWS had a greater number of small, unfilled adipocytes whereas HWS had a fewer number of unfilled cells. In response to force-feeding, the LWS chickens accommodated the increased energy through expansion of pre-existing adipocytes whereas the HWS, having fewer unfilled cells, generated new cells to accommodate the new lipids. It is intriguing that in our study with juveniles, the HWS had already reached the point where the abdominal fat contained primarily filled adipocytes, with very few unfilled cells. However, the average size of the fat cell was similar between depots. The average size of the fat cell was similar between all depots within the lines, which was unexpected given the differences in gene expression and differences in metabolism reported for visceral vs. subcutaneous fat in mammals. Further studies will investigate the developmental regulation of adipose tissue expansion in HWS and LWS.

Table 5.1 Adipocyte cellularity in 65-day-old male HWS and LWS chickens in abdominal fat and clavicular fat.

		Mean Area	Mean EqDiameter	Mean Circularity	Density
Abdominal fat (n=9)	HWS	3102.908	58.151	0.660	286.639
	LWS	1022.801	33.939	0.638	828.395
	SEM	53.627	0.633	0.008	14.921
	P-value	**<0.0001**	**<0.0001**	0.108	**<0.0001**
Clavicular fat (n=9)	HWS	3499.267	61.956	0.643	253.134
	LWS	1157.621	35.746	0.651	717.500
	SEM	69.596	0.839	0.011	20.261
	P-value	**<0.0001**	**<0.0001**	0.645	**<0.0001**

Data shown are least squares means ± standard errors of the means.

Table 5.2 Adipocyte cellularity in different adipose tissue depots from 65-day-old male HWS and LWS chickens.

		Mean Area	Mean EqDiameter	Mean Circularity	Density
HWS (n=9)	Abdominal fat	3102.908	58.151	0.660	286.639
	Clavicular fat	3499.267	61.956	0.643	253.134
	Subcutaneous fat	2770.616	55.032	0.612	307.160
	SEM	67.943	0.656	0.011	6.897
	P-value	**<0.0001**	**<0.0001**	**0.007**	**<0.0001**
LWS (n=9)	Abdominal fat	1022.801	33.939	0.638	828.395
	Clavicular fat	1157.621	35.746	0.651	717.500
	SEM	53.088	0.811	0.008	29.010
	P-value	0.068	0.109	0.256	**0.009**

Data shown are least squares means ± standard errors of the means.

(A)

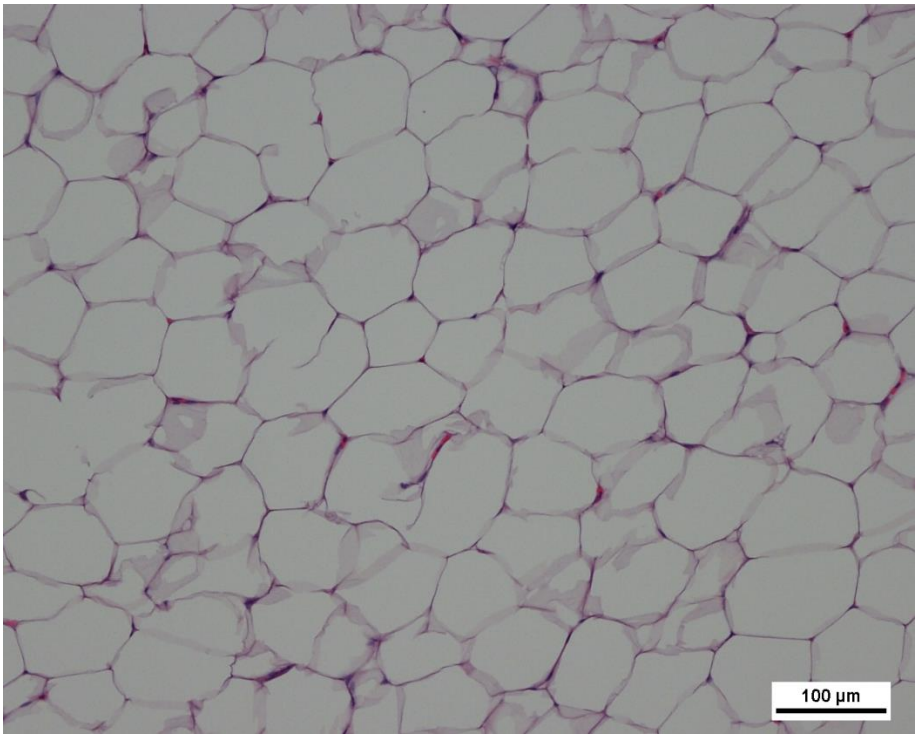

(B)

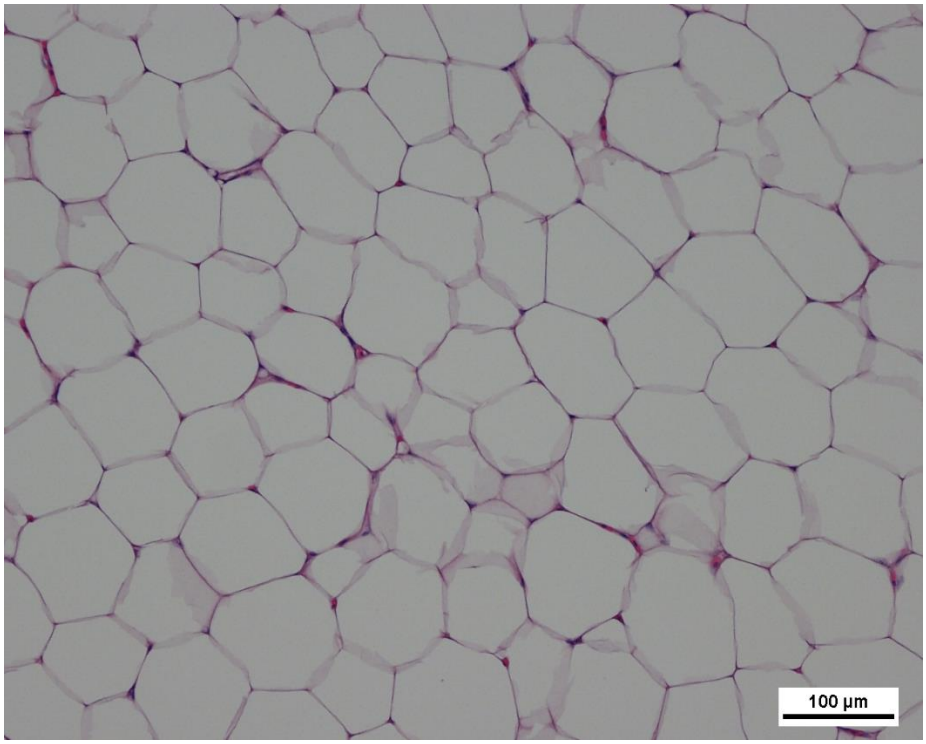

(C)

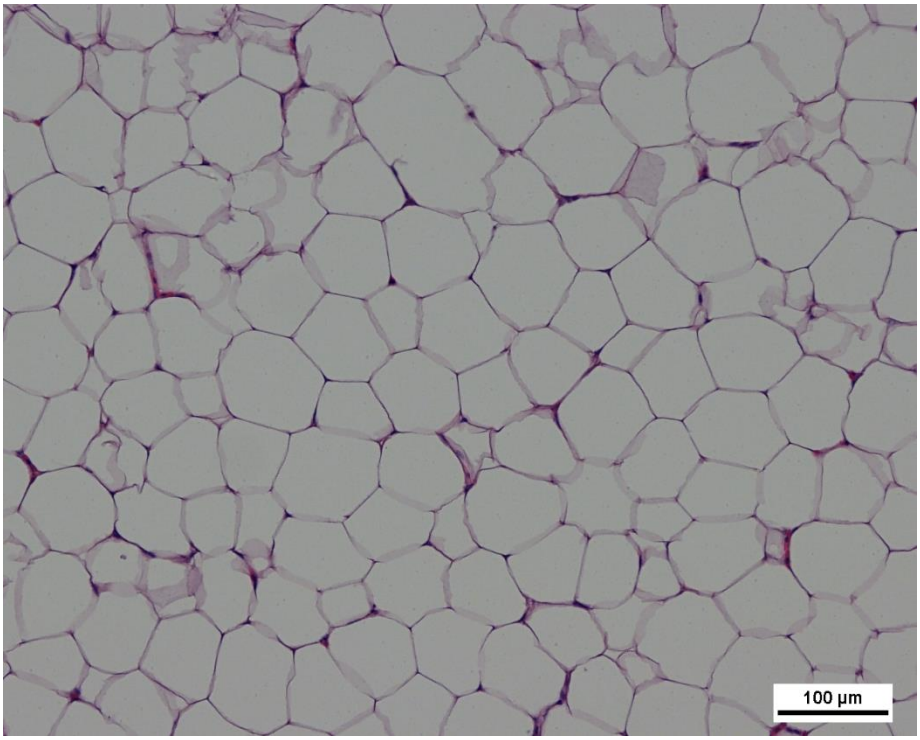

(D)

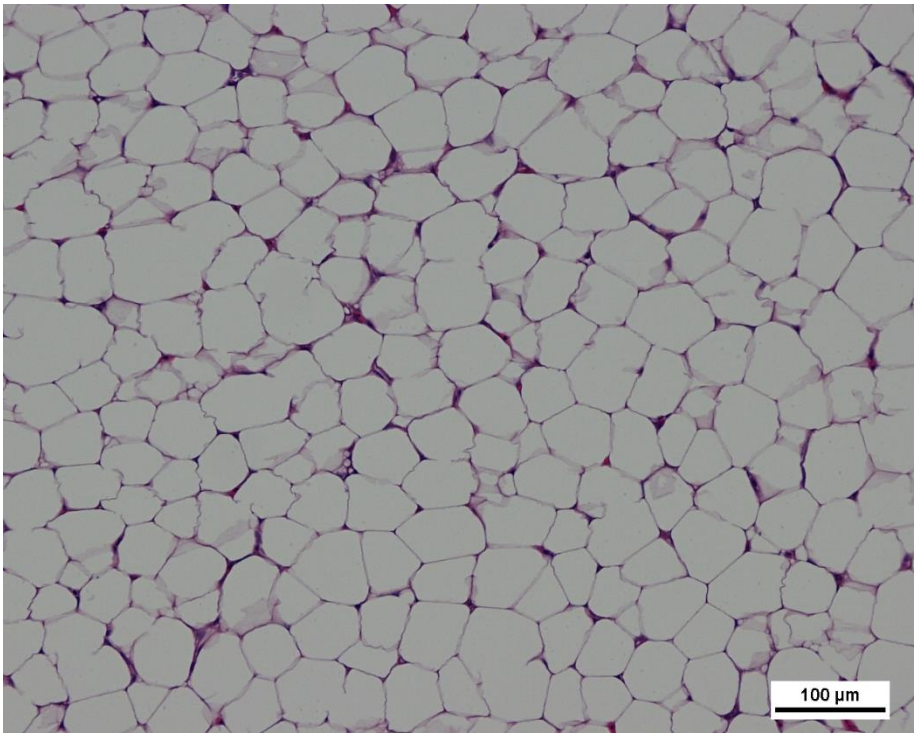

(E)

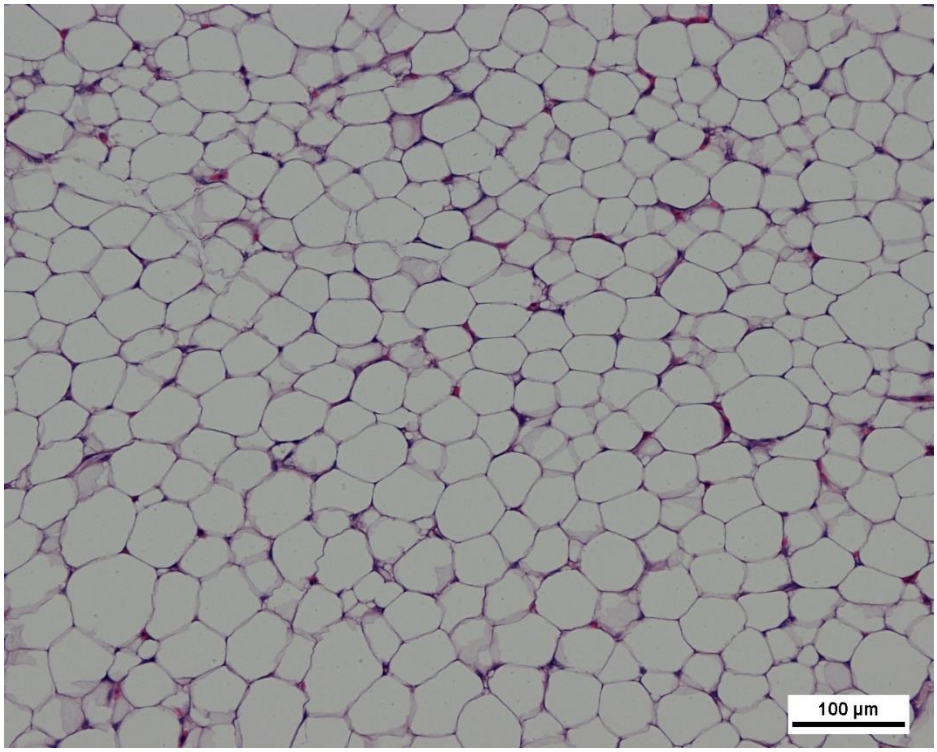

Figure 5.1 Adipose tissue histology of 65-day-old male HWS and LWS chickens. A) Abdominal fat of HWS chicken. B) Clavicular fat of HWS chicken. C) Subcutaneous fat of HWS chicken. D) Abdominal fat of LWS chicken. E) Clavicular fat of LWS chicken.

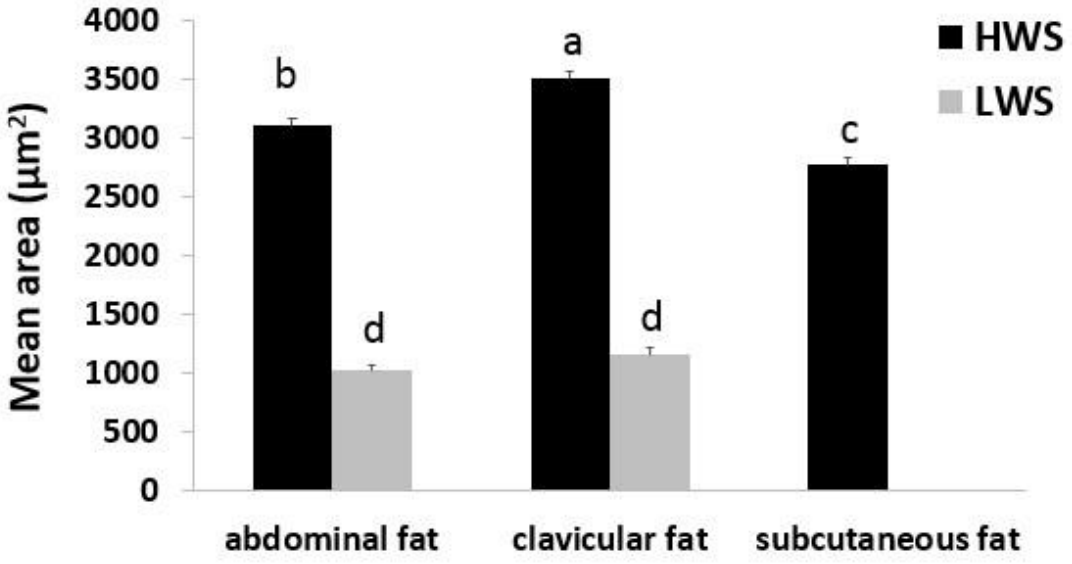

Figure 5.2 Mean area (µm^2) of adipocytes in abdominal fat, clavicular fat and subcutaneous fat from 65-day-old male HWS and LWS chickens. n=9. Bars with different letters represent significant differences, $P < 0.05$. Values represent least squares means ± SEM.

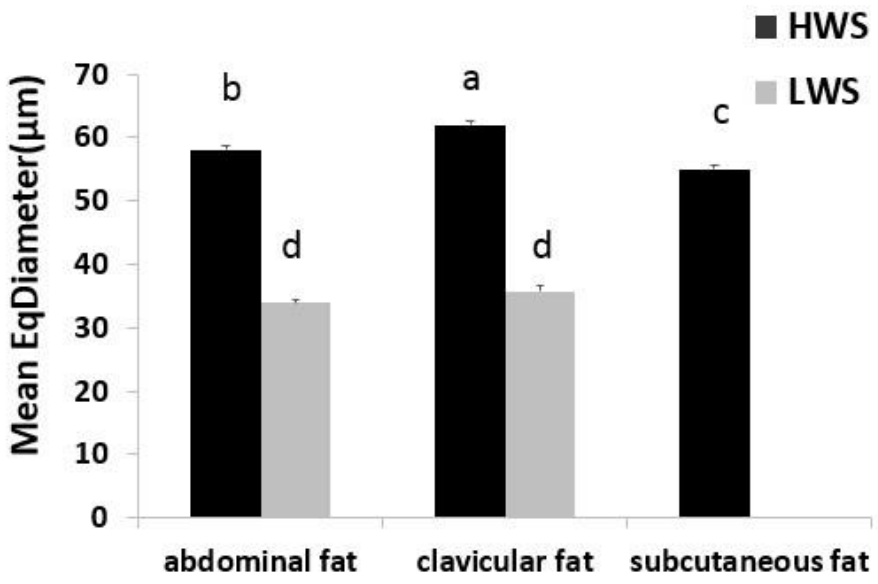

Figure 5.3 Mean equivalent diameter (μm) of adipocytes in abdominal fat, clavicular fat and subcutaneous fat from 65-day-old male HWS and LWS chickens. n=9. Bars with different letters represent significant differences, $P < 0.05$. Values represent least squares means ± SEM.

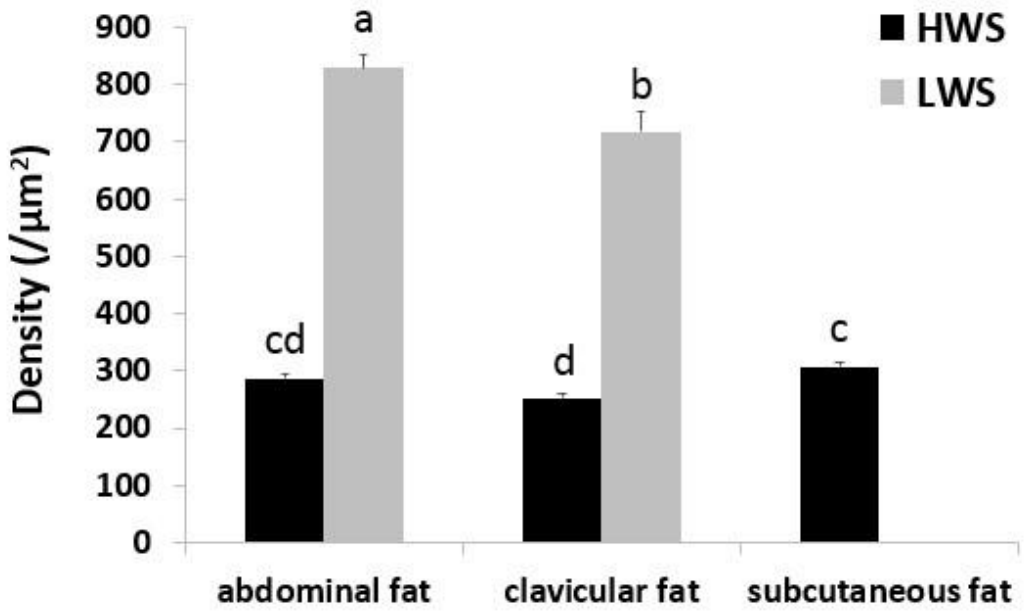

Figure 5.4 Adipocyte density (/μm^2) in abdominal fat, clavicular fat and subcutaneous fat from 65-day-old male HWS and LWS chickens. n=9. Bars with different letters represent significant differences, $P < 0.05$. Values represent least squares means ± SEM.

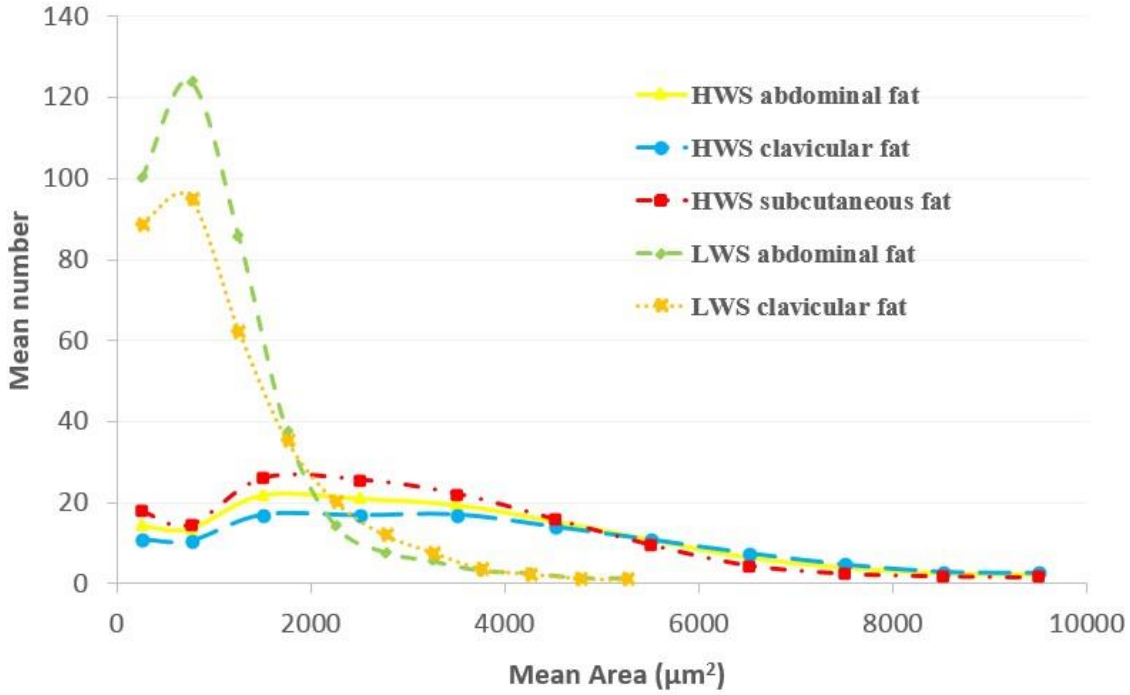

Figure 5.5 Adipocyte size distribution in different adipose tissues of 65-day-old male HWS and LWS chickens. n=9. Values represent mean numbers of adipocytes of a certain area (μm^2).

CHAPTER 6 Epilogue

6.1 Summary of thesis

In conclusion, the underlying mechanisms in the complex network that regulates energy homeostasis are critical to understand in the research of obesity and metabolic syndrome. The Virginia chicken lines, which show differences in feeding behavior and body composition, represent a model for evaluating mechanisms underlying the regulation of energy balance in anorexic vs. obese individuals. Results from our study suggest that in the relatively hypophagic and lean chickens, an enhanced ability to utilize fatty acids for energy and efficiently oxidize excess energy, prevents the accumulation of white adipose tissue, and greater fatty acid oxidation in the hypothalamus may indicate that the fuel sensing status in LWS is disrupted such that satiety-inducing signals predominate in appetite control. Greater metabolic flexibility in the skeletal muscle of the LWS is also consistent with superior oxidative efficiency and capacity to oxidize lipids. Differences in metabolism were also associated with differences in gene expression in adipose tissue and skeletal muscle of several genes that encode factors involved in PDC regulation that play an essential role in glucose and lipid metabolism (Figure 6). Information from this study may be useful in elucidating the molecular mechanisms underlying obesity and metabolic disorders. Results also can be extrapolated to agricultural production in the understanding of factors regulating the amount of lipid deposition in chicken carcass fat.

6.2 Future work

As our data were collected from chickens in the fasted state, results may differ in birds sampled during other nutritional states. Further studies can focus on other nutritional factors such as dietary fat content and composition. As supplemental studies, we can measure and compare the body composition of HWS and LWS chickens between hatch and sexual maturity. This may help us better understand the metabolic and gene expression differences between these two chicken lines at different ages. Our gene expression assays provided mRNA data. The post-transcriptional regulation and post-translational regulation may also be vital for expression and function of these factors. We can use Western blots to further analyze gene expression at the protein level. Furthermore, we can culture adipocytes from HWS and LWS chickens and use an in vitro model to understand the factors regulating adipocyte differentiation and metabolism. The final goal of our research is to study the nutritional regulation of energy metabolism in the hypothalamus, muscle and fat of lean and obese individuals, to provide information that can be beneficial to improve human body composition and reduce the occurrence of obesity and metabolic disorders.

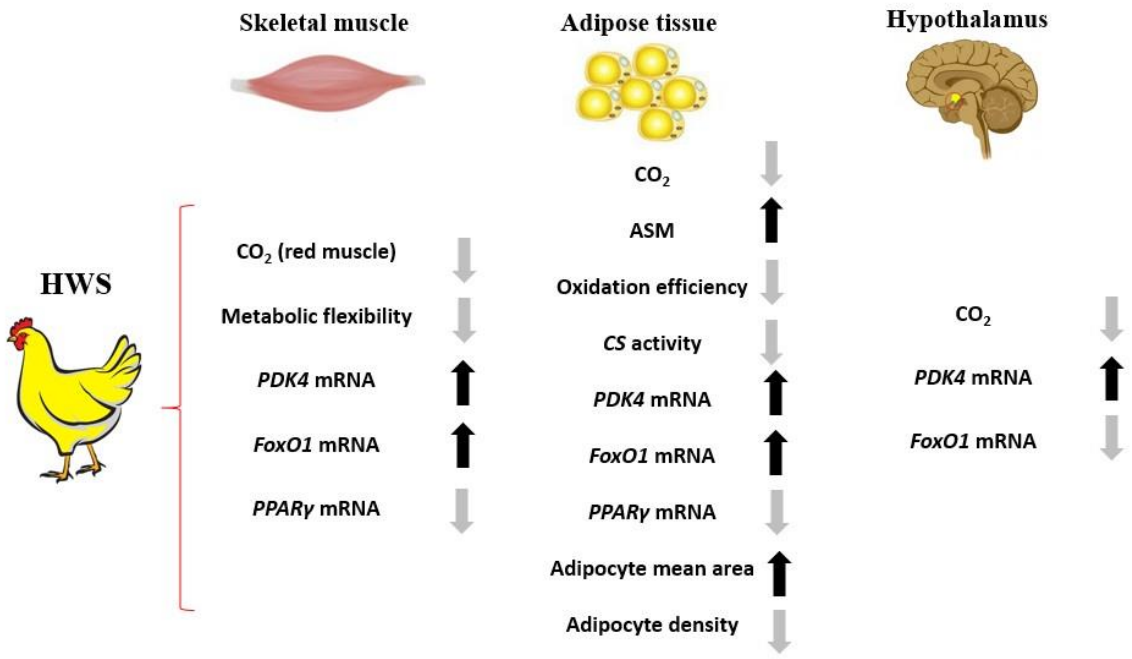

Figure 6 HWS chickens showed relative impairment in fatty acid oxidation efficiency and metabolic flexibility in both skeletal muscle and white adipose tissue. This was associated with differential expression of several genes, such as *PDK4*, *FoxO1* and *PPARγ*, and differences in adipocyte cellularity.

LITERATURE CITED

Accili, D. and K. C. Arden (2004). FoxOs at the crossroads of cellular metabolism, differentiation, and transformation. Cell **117**(4): 421-426.

Akhmedov, D., et al. (2012). Pyruvate dehydrogenase E1alpha phosphorylation is induced by glucose but does not control metabolism-secretion coupling in INS-1E clonal beta-cells. Biochimica et biophysica acta **1823**(10): 1815-1824.

Anderson, A. S., et al. (2013). Metabolic changes during ovarian cancer progression as targets for sphingosine treatment. Experimental cell research **319**(10): 1431-1442.

Araki, M. and K. Motojima (2006). Identification of ERRalpha as a specific partner of PGC-1alpha for the activation of PDK4 gene expression in muscle. The FEBS journal **273**(8): 1669-1680.

Arumugam, R., et al. (2010). Regulation of islet beta-cell pyruvate metabolism: interactions of prolactin, glucose, and dexamethasone. Endocrinology **151**(7): 3074-3083.

Ashmore, C. R. and L. Doerr (1971). Postnatal development of fiber types in normal and dystrophic skeletal muscle of the chick. Experimental neurology **30**(3): 431-446.

Attia, R. R., et al. (2010). Regulation of pyruvate dehydrogenase kinase 4 (PDK4) by thyroid hormone: role of the peroxisome proliferator-activated receptor gamma coactivator (PGC-1 alpha). The Journal of biological chemistry **285**(4): 2375-2385.

Barres, R., et al. (2009). Non-CpG methylation of the PGC-1alpha promoter through DNMT3B controls mitochondrial density. Cell metabolism **10**(3): 189-198.

Breton, C. (2013). The hypothalamus-adipose axis is a key target of developmental programming by maternal nutritional manipulation. The Journal of endocrinology **216**(2): R19-31.

Brons, C., et al. (2010). Deoxyribonucleic acid methylation and gene expression of PPARGC1A in human muscle is influenced by high-fat overfeeding in a birth-weight-dependent manner. The Journal of clinical endocrinology and metabolism **95**(6): 3048-3056.

Cadoudal, T., et al. (2008). Pyruvate dehydrogenase kinase 4: regulation by thiazolidinediones and implication in glyceroneogenesis in adipose tissue. Diabetes **57**(9): 2272-2279.

Calabotta, D. F., et al. (1985). Lipogenesis and lipolysis in fed and fasted chicks from high and low body weight lines. Poultry science **64**(4): 700-704.

Catoire, M., et al. (2012). Pronounced effects of acute endurance exercise on gene expression in resting and exercising human skeletal muscle. PloS one **7**(11): e51066.

Caton, P. W., et al. (2011). PPARalpha-LXR as a novel metabolostatic signalling axis in skeletal muscle that acts to optimize substrate selection in response to nutrient status. The Biochemical journal **437**(3): 521-530.

Connaughton, S., et al. (2010). Regulation of pyruvate dehydrogenase kinase isoform 4 (PDK4) gene expression by glucocorticoids and insulin. Molecular and cellular endocrinology **315**(1-2): 159-167.

Constantin-Teodosiu, D., et al. (2012). The role of FOXO and PPAR transcription factors in diet-mediated inhibition of PDC activation and carbohydrate oxidation during

exercise in humans and the role of pharmacological activation of PDC in overriding these changes. Diabetes **61**(5): 1017-1024.

de Lange, P., et al. (2007). Fuel economy in food-deprived skeletal muscle: signaling pathways and regulatory mechanisms. FASEB journal : official publication of the Federation of American Societies for Experimental Biology **21**(13): 3431-3441.

Ding, F., et al. (2010). Neonatal maternal deprivation response and developmental changes in gene expression revealed by hypothalamic gene expression profiling in mice. PloS one **5**(2): e9402.

Dunnington, E. A., et al. (2013). Phenotypic responses of chickens to long-term, bidirectional selection for juvenile body weight--historical perspective. Poultry science **92**(7): 1724-1734.

Dunnington, E. A. and P. B. Siegel (1996). Long-term divergent selection for eight-week body weight in white Plymouth rock chickens. Poultry science **75**(10): 1168-1179.

Eivers, S. S., et al. (2012). PGC-1alpha encoded by the PPARGC1A gene regulates oxidative energy metabolism in equine skeletal muscle during exercise. Animal genetics **43**(2): 153-162.

Frisard, M. I., et al. (2010). Toll-like receptor 4 modulates skeletal muscle substrate metabolism. American journal of physiology. Endocrinology and metabolism **298**(5): E988-998.

Furuyama, T., et al. (2003). Forkhead transcription factor FOXO1 (FKHR)-dependent induction of PDK4 gene expression in skeletal muscle during energy deprivation. The Biochemical journal **375**(Pt 2): 365-371.

Galgani, J. E., et al. (2008). Metabolic flexibility and insulin resistance. American journal of physiology. Endocrinology and metabolism **295**(5): E1009-1017.

Gross, D. N., et al. (2008). The role of FoxO in the regulation of metabolism. Oncogene **27**(16): 2320-2336.

Guarente, L. and C. Kenyon (2000). Genetic pathways that regulate ageing in model organisms. Nature **408**(6809): 255-262.

Gudi, R., et al. (1995). Diversity of the pyruvate dehydrogenase kinase gene family in humans. The Journal of biological chemistry **270**(48): 28989-28994.

Hagen, C. J., et al. (2013). Stimulation of food intake after central galanin is associated with arcuate nucleus activation and does not differ between genetically selected low and high body weight lines of chickens. Neuropeptides **47**(4): 281-285.

Hamdy, O., et al. (2006). Metabolic obesity: the paradox between visceral and subcutaneous fat. Current diabetes reviews **2**(4): 367-373.

Herbst, E. A., et al. (2012). Role of pyruvate dehydrogenase kinase 4 in regulating PDH activation during acute muscle contraction. Applied physiology, nutrition, and metabolism = Physiologie appliquee, nutrition et metabolisme **37**(1): 48-52.

Holloway, G. P., et al. (2010). Compensatory increases in nuclear PGC1alpha protein are primarily associated with subsarcolemmal mitochondrial adaptations in ZDF rats. Diabetes **59**(4): 819-828.

Holness, M. J., et al. (2000). Targeted upregulation of pyruvate dehydrogenase kinase (PDK)-4 in slow-twitch skeletal muscle underlies the stable modification of the regulatory characteristics of PDK induced by high-fat feeding. Diabetes **49**(5): 775-781.

Holness, M. J. and M. C. Sugden (2003). Regulation of pyruvate dehydrogenase complex activity by reversible phosphorylation. Biochemical Society transactions **31**(Pt 6): 1143-1151.

Holness, M. J., et al. (2012). Adipocyte pyruvate dehydrogenase kinase 4 expression is associated with augmented PPARgamma upregulation in early-life programming of later obesity. FEBS open bio **2**: 32-36.

Hsu, P. P. and D. M. Sabatini (2008). Cancer cell metabolism: Warburg and beyond. Cell **134**(5): 703-707.

Huang, B., et al. (2003). Starvation and diabetes reduce the amount of pyruvate dehydrogenase phosphatase in rat heart and kidney. Diabetes **52**(6): 1371-1376.

Hwang, B., et al. (2009). Pyruvate dehydrogenase kinase isoenzyme 4 (PDHK4) deficiency attenuates the long-term negative effects of a high-saturated fat diet. The Biochemical journal **423**(2): 243-252.

Hwang, B., et al. (2012). Additive effects of clofibric acid and pyruvate dehydrogenase kinase isoenzyme 4 (PDK4) deficiency on hepatic steatosis in mice fed a high saturated fat diet. The FEBS journal **279**(10): 1883-1893.

Jeong, J. Y., et al. (2012). Transcriptional regulation of pyruvate dehydrogenase kinase. Diabetes & metabolism journal **36**(5): 328-335.

Jeoung, N. H. and R. A. Harris (2008). Pyruvate dehydrogenase kinase-4 deficiency lowers blood glucose and improves glucose tolerance in diet-induced obese mice. American journal of physiology. Endocrinology and metabolism **295**(1): E46-54.

Jeoung, N. H. and R. A. Harris (2010). Role of pyruvate dehydrogenase kinase 4 in regulation of blood glucose levels. Korean diabetes journal **34**(5): 274-283.

Jeoung, N. H., et al. (2006). Role of pyruvate dehydrogenase kinase isoenzyme 4 (PDHK4) in glucose homoeostasis during starvation. The Biochemical journal **397**(3): 417-425.

Jha, M. K., et al. (2012). Pyruvate Dehydrogenase Kinases in the Nervous System: Their Principal Functions in Neuronal-glial Metabolic Interaction and Neuro-metabolic Disorders. Current neuropharmacology **10**(4): 393-403.

Ka, S., et al. (2013). Expression of carnitine palmitoyl-CoA transferase-1B is influenced by a cis-acting eQTL in two chicken lines selected for high and low body weight. Physiological genomics **45**(9): 367-376.

Kase, E. T., et al. (2005). Skeletal muscle lipid accumulation in type 2 diabetes may involve the liver X receptor pathway. Diabetes **54**(4): 1108-1115.

Kelley, D. E. and L. J. Mandarino (2000). Fuel selection in human skeletal muscle in insulin resistance: a reexamination. Diabetes **49**(5): 677-683.

Kim, Y. D., et al. (2012). Metformin inhibits growth hormone-mediated hepatic PDK4 gene expression through induction of orphan nuclear receptor small heterodimer partner. Diabetes **61**(10): 2484-2494.

Kim, Y. I., et al. (2006). Insulin regulation of skeletal muscle PDK4 mRNA expression is impaired in acute insulin-resistant states. Diabetes **55**(8): 2311-2317.

Kulkarni, S. S., et al. (2012). Mitochondrial regulators of fatty acid metabolism reflect metabolic dysfunction in type 2 diabetes mellitus. Metabolism: clinical and experimental **61**(2): 175-185.

Kwon, H. S. and R. A. Harris (2004). Mechanisms responsible for regulation of pyruvate dehydrogenase kinase 4 gene expression. Adv Enzyme Regul **44**: 109-121.

Larsen, S., et al. (2012). Biomarkers of mitochondrial content in skeletal muscle of healthy young human subjects. The Journal of physiology **590**(Pt 14): 3349-3360.

Lin, J. D. (2009). Minireview: the PGC-1 coactivator networks: chromatin-remodeling and mitochondrial energy metabolism. Mol Endocrinol **23**(1): 2-10.

Livak, K. J. and T. D. Schmittgen (2001). Analysis of relative gene expression data using real-time quantitative PCR and the 2(-Delta Delta C(T)) Method. Methods **25**(4): 402-408.

Lopaschuk, G. D., et al. (2010). Targeting intermediary metabolism in the hypothalamus as a mechanism to regulate appetite. Pharmacological reviews **62**(2): 237-264.

Lopez, M. and A. Vidal-Puig (2008). Brain lipogenesis and regulation of energy metabolism. Curr Opin Clin Nutr Metab Care **11**(4): 483-490.

Maffeis, C., et al. (2007). Fat cell size, insulin sensitivity, and inflammation in obese children. The Journal of pediatrics **151**(6): 647-652.

March, B. E. and G. Hansen (1977). Lipid accumulation and cell multiplication in adipose bodies in White Leghorn and broiler-type chicks. Poultry science **56**(3): 886-894.

Marquez, G. C., et al. (2010). Genetic diversity and population structure of American Red Angus cattle. Journal of animal science **88**(1): 59-68.

Matsuzawa, Y., et al. (1995). Pathophysiology and pathogenesis of visceral fat obesity. Obesity research **3 Suppl 2**: 187S-194S.

Meijer, K., et al. (2011). Human primary adipocytes exhibit immune cell function: adipocytes prime inflammation independent of macrophages. PloS one **6**(3): e17154.

Michelakis, E. D., et al. (2010). Metabolic modulation of glioblastoma with dichloroacetate. Science translational medicine **2**(31): 31ra34.

Mori, J., et al. (2013). ANG II causes insulin resistance and induces cardiac metabolic switch and inefficiency: a critical role of PDK4. American journal of physiology. Heart and circulatory physiology **304**(8): H1103-1113.

Morrell, J. A., et al. (2003). AZD7545 is a selective inhibitor of pyruvate dehydrogenase kinase 2. Biochemical Society transactions **31**(Pt 6): 1168-1170.

Morton, G. J., et al. (2006). Central nervous system control of food intake and body weight. Nature **443**(7109): 289-295.

Nahle, Z., et al. (2008). CD36-dependent regulation of muscle FoxO1 and PDK4 in the PPAR delta/beta-mediated adaptation to metabolic stress. The Journal of biological chemistry **283**(21): 14317-14326.

Nakai, N., et al. (2000). The abundance of mRNAs for pyruvate dehydrogenase kinase isoenzymes in brain regions of young and aged rats. Life sciences **68**(5): 497-503.

Nellemann, B., et al. (2013). Growth hormone-induced insulin resistance in human subjects involves reduced pyruvate dehydrogenase activity. Acta physiologica.

Newmyer, B. A., et al. (2013). Neuropeptide Y is associated with changes in appetite-associated hypothalamic nuclei but not food intake in a hypophagic avian model. Behavioural brain research **236**(1): 327-331.

Nye, C. K., et al. (2008). Glyceroneogenesis is the dominant pathway for triglyceride glycerol synthesis in vivo in the rat. The Journal of biological chemistry **283**(41): 27565-27574.

Pilegaard, H. and P. D. Neufer (2004). Transcriptional regulation of pyruvate dehydrogenase kinase 4 in skeletal muscle during and after exercise. The Proceedings of the Nutrition Society **63**(2): 221-226.

Poirier, P., et al. (2006). Obesity and cardiovascular disease: pathophysiology, evaluation, and effect of weight loss: an update of the 1997 American Heart Association Scientific Statement on Obesity and Heart Disease from the Obesity Committee of the Council on Nutrition, Physical Activity, and Metabolism. Circulation **113**(6): 898-918.

Poplawski, M. M., et al. (2010). Hypothalamic responses to fasting indicate metabolic reprogramming away from glycolysis toward lipid oxidation. Endocrinology **151**(11): 5206-5217.

Postic, C., et al. (2004). Role of the liver in the control of carbohydrate and lipid homeostasis. Diabetes Metab **30**(5): 398-408.

Power, R. A., et al. (2007). Carnitine revisited: potential use as adjunctive treatment in diabetes. Diabetologia **50**(4): 824-832.

Puelles, L. (2007). The chick brain in stereotaxic coordinates : an atlas featuring neuromeric subdivisions and mammalian homologies. Amsterdam ; Boston, Academic Press.

Puigserver, P. and B. M. Spiegelman (2003). Peroxisome proliferator-activated receptor-gamma coactivator 1 alpha (PGC-1 alpha): transcriptional coactivator and metabolic regulator. Endocr Rev **24**(1): 78-90.

Randle, P. J. (1986). Fuel selection in animals. Biochemical Society transactions **14**(5): 799-806.

Randle, P. J. (1998). Regulatory interactions between lipids and carbohydrates: the glucose fatty acid cycle after 35 years. Diabetes/metabolism reviews **14**(4): 263-283.

Rinnankoski-Tuikka, R., et al. (2012). Effects of high-fat diet and physical activity on pyruvate dehydrogenase kinase-4 in mouse skeletal muscle. Nutrition & metabolism **9**(1): 53.

Robey, W. W., et al. (1988). Hyperplastic response of adipose tissue to caloric overconsumption in sexually mature chickens. Poultry science **67**(5): 800-808.

Robey, W. W., et al. (1992). Adipocyte dynamics in the retroperitioneal fat depot of genetically selected adult high- and low-weight line chickens. Arch. Gerflugelk **56**(2): 68-72.

Roche, T. E. and Y. Hiromasa (2007). Pyruvate dehydrogenase kinase regulatory mechanisms and inhibition in treating diabetes, heart ischemia, and cancer. Cellular and molecular life sciences : CMLS **64**(7-8): 830-849.

Schaffler, A., et al. (2005). Hypothesis paper Brain talks with fat--evidence for a hypothalamic-pituitary-adipose axis? Neuropeptides **39**(4): 363-367.

Sears, D. D., et al. (2007). Selective modulation of promoter recruitment and transcriptional activity of PPARgamma. Biochemical and biophysical research communications **364**(3): 515-521.

Serra, D., et al. (2013). Mitochondrial fatty acid oxidation in obesity. Antioxidants & redox signaling **19**(3): 269-284.

Shimizu, H. and M. Mori (2005). The brain-adipose axis: a review of involvement of molecules. Nutritional neuroscience **8**(1): 7-20.

Song, S., et al. (2010). Peroxisome proliferator activated receptor alpha (PPARalpha) and PPAR gamma coactivator (PGC-1alpha) induce carnitine palmitoyltransferase IA (CPT-1A) via independent gene elements. Mol Cell Endocrinol **325**(1-2): 54-63.

Stacpoole, P. W., et al. (1998). Clinical pharmacology and toxicology of dichloroacetate. Environmental health perspectives **106 Suppl 4**: 989-994.

Storlien, L., et al. (2004). Metabolic flexibility. The Proceedings of the Nutrition Society **63**(2): 363-368.

Strumilo, S. (2005). Short-term regulation of the mammalian pyruvate dehydrogenase complex. Acta biochimica Polonica **52**(4): 759-764.

Sugden, M. C. (2003). PDK4: A factor in fatness? Obesity research **11**(2): 167-169.

Sugden, M. C. and M. J. Holness (1994). Interactive regulation of the pyruvate dehydrogenase complex and the carnitine palmitoyltransferase system. FASEB journal : official publication of the Federation of American Societies for Experimental Biology **8**(1): 54-61.

Sugden, M. C. and M. J. Holness (2006). Mechanisms underlying regulation of the expression and activities of the mammalian pyruvate dehydrogenase kinases. Archives of physiology and biochemistry **112**(3): 139-149.

Sugden, M. C., et al. (2000). Fibre-type specific modification of the activity and regulation of skeletal muscle pyruvate dehydrogenase kinase (PDK) by prolonged starvation and refeeding is associated with targeted regulation of PDK isoenzyme 4 expression. The Biochemical journal **346 Pt 3**: 651-657.

Sugden, M. C., et al. (2009). PPARs and the orchestration of metabolic fuel selection. Pharmacological research : the official journal of the Italian Pharmacological Society **60**(3): 141-150.

Sun, K., et al. (2011). Adipose tissue remodeling and obesity. The Journal of clinical investigation **121**(6): 2094-2101.

Sutendra, G. and E. D. Michelakis (2013). Pyruvate dehydrogenase kinase as a novel therapeutic target in oncology. Frontiers in oncology **3**: 38.

Tao, R., et al. (2013). Genetic inactivation of pyruvate dehydrogenase kinases improves hepatic insulin resistance induced diabetes. PloS one **8**(8): e71997.

Wallace, M., et al. (2013). Metabolomic analysis of pancreatic beta cells following exposure to high glucose. Biochimica et biophysica acta **1830**(3): 2583-2590.

Wan, Z., et al. (2012). Epinephrine induces PDK4 mRNA expression in adipose tissue from obese, insulin resistant rats. Obesity **20**(2): 453-456.

Wan, Z., et al. (2010). Epinephrine-mediated regulation of PDK4 mRNA in rat adipose tissue. American journal of physiology. Cell physiology **299**(5): C1162-1170.

Wende, A. R., et al. (2005). PGC-1alpha coactivates PDK4 gene expression via the orphan nuclear receptor ERRalpha: a mechanism for transcriptional control of muscle glucose metabolism. Molecular and cellular biology **25**(24): 10684-10694.

Wu, C. A., et al. (2013). Nutrient deprivation induces the Warburg effect through ROS/AMPK-dependent activation of pyruvate dehydrogenase kinase. Biochimica et biophysica acta **1833**(5): 1147-1156.

Wu, P., et al. (1999). Mechanism responsible for inactivation of skeletal muscle pyruvate dehydrogenase complex in starvation and diabetes. Diabetes **48**(8): 1593-1599.

Xu, J., et al. (2006). Regulation of PDK mRNA by high fatty acid and glucose in pancreatic islets. Biochemical and biophysical research communications **344**(3): 827-833.

Xu, P., et al. (2011). Genetic selection for body weight in chickens has altered responses of the brain's AMPK system to food intake regulation effect of ghrelin, but not obestatin. Behavioural brain research **221**(1): 216-226.

Yao, J., et al. (2009). Mitochondrial bioenergetic deficit precedes Alzheimer's pathology in female mouse model of Alzheimer's disease. Proceedings of the National Academy of Sciences of the United States of America **106**(34): 14670-14675.

Zhang, L., et al. (2012). Activating cardiac E2F1 induces up-regulation of pyruvate dehydrogenase kinase 4 in mice on a short term of high fat feeding. FEBS letters **586**(7): 996-1003.

Zhao, G., et al. (2008). Overexpression of pyruvate dehydrogenase kinase 4 in heart perturbs metabolism and exacerbates calcineurin-induced cardiomyopathy. American journal of physiology. Heart and circulatory physiology **294**(2): H936-943.